HJ-Gauss

Monte-Carlo Hamilton-Jacobi Reachability

Full Exposition: From TVD-RK Levelsets to Monte Carlo Sampling for BRTs.

Lekan Molu · Amazon IRG

Amazon Robotics · August 18, 2026

with V. Renganathan (Cranfield) and N. Cho (Seoul National University)

🎯 BLUF (Bottom Line Up Front) - (1/2)

Grid-resolved Hamilton-Jacobi (HJ) BRTs yield certified safety sets at a $O(M^n)$ memory cost.

- 🧱 **Background:** LevelSetPy resolves backward reachable sets/tubes by discretizing the HJ PDE (upwinding + Lax-Friedrichs + TVD-RK) on a grid — certified, but exponential in state dimension n.
- 🌊 **Idea:** a Cole-Hopf transformation turns the *viscous* HJ PDE into a **linear heat equation**; Feynman-Kac evaluates it as a **Gaussian expectation**. No grid.

HJ-Gauss replaces the grid with Gaussian Monte-Carlo, dropping the footprint to $O(N \cdot n)$.

🎯 BLUF (Bottom Line Up Front) - (2/2)

> **HJ-Gauss replaces the grid with Gaussian Monte-Carlo, dropping the footprint to $O(N \cdot n)$.**

- 🔁 **Generality:** a frozen-coefficient **Picard iteration** handles the nonconvex, state-dependent Hamiltonians of reachability.
- 📐 **Rigor:** $O(N^{-1/2})$ concentration, contraction convergence, a linearization residual bound, and a **conservative safety certificate**.
- 🤖 **For this room:** the windowed reachable tube is a dynamics-aware **conflict predicate** for MAPF; the value gradient is a **score** for diffusion planners.

> **This Gaussian kernel is the diffusion kernel, the bridge to learning-based planners.**

🧭 Roadmap — Parts 0-6

Part	Theme
0	Framing, significance, notation
1	Hamilton-Jacobi PDE theory & viscosity solutions
2	Reachability & safety foundations
3	The grid pipeline: LevelSetPy numerics
4	The wall: curse of dimensionality & prior grid-free work
5	HJ-Gauss core theory: Cole-Hopf → heat → Feynman-Kac → Picard
6	Importance sampling & variance control

▶ **Continue:** Parts 7-12 on the next slide.

🧭 Roadmap — Parts 7-12

Part	Theme
7	Guarantees: concentration, contraction, residual, certificate
8	Experiments from the paper (rockets, Dubins, 45D, 10^5 birds)
9	Application: multi-agent path finding (AMFS)
10	The diffusion connection
11	Dirty Laundry: limits & boundaries
12	Conclusions, future work, references

📏 Notations

Symbol	Meaning
$x \in \Omega \subseteq \mathbb{R}^n$	x: State; Ω: Open set; n = State dimension
$v(t, x)$	Value function; v_t time derivative; $Dv = \nabla_x v$ spatial gradient (co-state)
$H(t; x, p)$	Hamiltonian; p = co-state
$g(x)$	Terminal/target datum (signed distance $\ell(x)$); BUC
$\delta > 0$	Viscosity parameter

📏 Notations

Symbol	Meaning
$\omega^\delta = e^{-cv^\delta}$	Cole-Hopf transformed variable
$c(t;x)$	Frozen coefficient $= \frac{2}{\delta} H^\delta / \lvert Dv^\delta \rvert^2$
$M,\ N$	Grid points per dimension (M); Monte-Carlo samples per query state (N)
$\mathcal{L}_0,\ \mathcal{L}$	Target set, backward reachable tube (BRT)

Two independent counts: M evaluation states (arbitrary, grid-free) vs N Gaussian samples drawn *per state*. Total randomness per iteration $= M \times N$.

👥 Who Should Care, and Why

- **Autonomous mobility / MAPF:** a certified, dynamics-aware, disturbance-robust conflict predicate that slots into rolling-horizon planners at fleet scale.
- **Safe RL / policy verification:** computing backward reachable tubes for a closed-loop learned policy is memory-bound on grids; $O(N \cdot n)$ lifts that bound.
- **Differential games / pursuit-evasion:** the adversarial worst-case reachable set is what HJ-Isaacs computes.

> The unifying object is a **value function whose sign certifies safety**. This talk is about computing that sign where grids cannot.

👥 Who Should Care, and Why

- **Differential games / pursuit-evasion:** the adversarial worst-case reachable set is what HJ-Isaacs computes.
- **Diffusion / generative planning:** the Cole-Hopf kernel *is* the score-based diffusion kernel; the value gradient is a score.
- **Air-traffic, collision avoidance, multi-robot control:** the classical application domain of HJ reachability.

> The unifying object is a **value function whose sign certifies safety**. This talk is about computing that sign where grids cannot.

Part 1

🧮 Hamilton-Jacobi PDE Theory Recap

Viscosity solutions, vanishing viscosity, and why we need them.

🧮 The Cauchy-Type HJ Equation

Our chief object is the evolution (Cauchy) HJ equation

$$v_t(x,t) + H(t; x, \nabla_x v) = 0 \ \text{ in } \Omega \times (0,T], \qquad v(x,0) = v_0(x) \ \text{ in } \Omega,$$

with $H : (0,T] \times \mathbb{R}^n \times \mathbb{R}^n \to \mathbb{R}$ continuous and g, v_0 **bounded, uniformly continuous (BUC)**.

- A closely related object is the **scalar conservation law / convection equation** $v_t + \sum_i f_i(v)_{x_i} = 0$, whose shock theory motivates the numerics.
- The HJ equation is **first-order, nonlinear, hyperbolic**.

> First-order nonlinear hyperbolic PDEs generically fail to have smooth global solutions — the reason the entire viscosity-solution apparatus exists.

🧮 Why Classical Solutions Fail: Crossing Characteristics

- The **method of characteristics** integrates the PDE along curves in (x, t).
- For nonlinear H, characteristics **cross**: multiple characteristics carry conflicting values to the same point → a **shock** / gradient discontinuity.
- Consequence: no global C^1 solution exists in general, **even when H and g are smooth**.
- Global analysis via classical PDE theory is "virtually impossible" (Crandall-Lions).

> The value function of a differential game develops **kinks and shocks** right at the barrier — the most safety-relevant region. We must define a *weak* solution that survives there.

🧮 Viscosity Solutions[1]

- **Viscosity solutions** are the correct weak solution class for HJ PDEs: they exist almost everywhere, and enjoy **existence, uniqueness, and stability** theorems.
- Definition (sketch) via test functions: v is a viscosity *subsolution* if for every smooth φ touching v from above at (x_0, t_0), $\varphi_t + H(\cdot, \nabla\varphi) \leq 0$; *supersolution* with the reverse inequality and touching from below; a **solution** is both.
- This selects the physically-correct kinked solution and discards spurious ones.

> Viscosity theory gives us a **unique** object to compute and to certify — indispensable for a safety guarantee.

[1] Crandall & Lions, 1983

🧮 Vanishing Viscosity

Introduce $\delta > 0$ and regularize (parabolic smoothing, as in gas dynamics):

$$v_t^\delta + H(t; x, \nabla v^\delta) = \tfrac{\delta}{2}\, \Delta v^\delta \ \text{ in } \Omega \times (0, T], \qquad v^\delta(x, 0) = g(x).$$

- The added Laplacian makes the PDE **parabolic**, hence classically well-posed: $v^\delta \in C^{2,1}$, unique, stable, BUC for all T.
- Traversing the limit $\delta \to 0$ recovers the unique viscosity solution.

> δ is the linchpin of HJ-Gauss: it is both the **smoothing** that admits a classical solution *and* the **diffusion coefficient** of the heat equation we are about to expose.

🧮 The Crandall-Lions Error Bound

The viscous solution approximates the inviscid viscosity solution at a known rate:

$$\sup_{t\in(0,T]} \sup_{x\in\mathbb{R}^n} \left| v(t,x) - v^\delta(t,x) \right| \le k\sqrt{\delta}, \qquad k > 0.$$

- **Bias scales as $O(\sqrt{\delta})$:** smaller δ → more accurate.
- But (preview) smaller δ → more concentrated exponential weights → higher Monte-Carlo variance.
- This is the **bias-variance knob** we will formalize in Part 7 ($\delta \sim N^{-1/3}$).

> One scalar δ trades geometric accuracy against sampling variance. Choosing it well is the practical art of the method.

🧮 Admissible Data on $\mathbb{R}^n$

- Whole-space heat theory requires the datum in $C(\mathbb{R}^n) \cap L^\infty(\mathbb{R}^n)$.
- The transformed datum is $\omega^\delta(0,\cdot) = e^{-c\,g}$ — **not** g itself. This matters: the signed distance ℓ is *unbounded above*, but for a bounded target $g \ge g_{\min}$ and $g \to +\infty$ as $|x| \to \infty$, so

$$0 < e^{-cg(y)} \le e^{-cg_{\min}}, \qquad e^{-cg(y)} \to 0 \text{ as } |y| \to \infty.$$

- Hence e^{-cg} is continuous, strictly positive, bounded, decaying → the heat solution is the **unique bounded** one, the integral converges absolutely, and the Gaussian expectation is genuine and **unbiased**.

> Only the **lower** bound $g \ge g_{\min}$ is needed; no upper bound on g is used. This is what lets us sample over all of $\mathbb{R}^n$.

Part 2

🛡️ Reachability & Safety Foundations

What a certified safety set *is*, before we compute one.

What Is Reachability?

- **Reachability** concerns the *decidability* of a dynamical system's trajectory evolution across a phase space.
- A reachable system is **decidable** when one can compute *all* states reachable from an initial condition **in a finite number of steps**.
- Dual questions:
  - **Forward:** where can the system go from here?
  - **Backward:** from which states is a target inevitably reached (or avoidable)?
- Safety analysis is naturally **backward**: characterize the set of states doomed to enter a danger set, then stay out of it.

> Certifying a learned controller, neural policy, or planner means proving it satisfies all specified requirements — a **verification** problem. Reachability is the geometric engine of that verification.

Backward Reachable Sets and Tubes

- **Backward Reachable Set (BRS):** states that reach the target at a *specific* time.
- **Backward Reachable Tube (BRT):** states that reach the target at *some* time in $[0, T]$ — the safety-relevant object.
- **Reach-Avoid Tube (BRAT):** states that can reach a goal while avoiding an obstacle set.
- **Robustly-Controlled BRT (RCBRT):** when the controller must counter a **worst-case disturbance** — the adversarial guarantee.

$$\mathcal{L}([-T, 0], \mathcal{L}_0) = \{x \in \mathbb{R}^n : \ \exists\, \beta \in \mathcal{B}(t)\ \forall\, u \in \mathcal{U}(t),\ \exists\, \bar{\tau} \in [-T, 0],\ \xi(\bar{\tau}) \in \mathcal{L}_0\}.$$

> The strategy structure ($\exists \beta\ \forall u$) encodes the game: disturbance plays a nonanticipative strategy β against control u.

🎓 Why "Backward" Reachable Sets

- A **continuous backward reachable set** is the set of all states from which trajectories can reach a given target set $G(0)$.
- Called **"backward"** to distinguish it from the *forward* reachable set.
- **To compute it, run the dynamics backward in time** from the target set.

> For safety, the target is usually the *unsafe* set, so the backward reachable set is the set of states doomed to become unsafe.

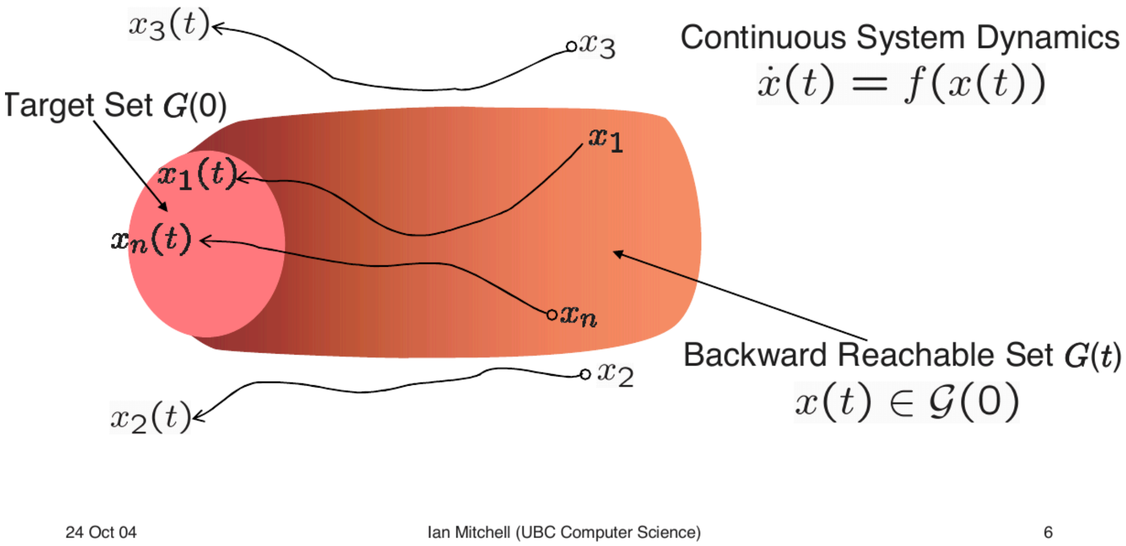

(Mitchell 2004, Reach Sets and the HJ Equation)

🎓 How to *Represent* the Set/Tube?

Computing a reachable set poses two coupled problems:

- **Represent** the set of reachable states.
- **Evolve** that set according to the dynamics.

Inset: A sphere as an SDF — LevelSetPy (L. Molu), ACM TOMS 51(2), 2025.

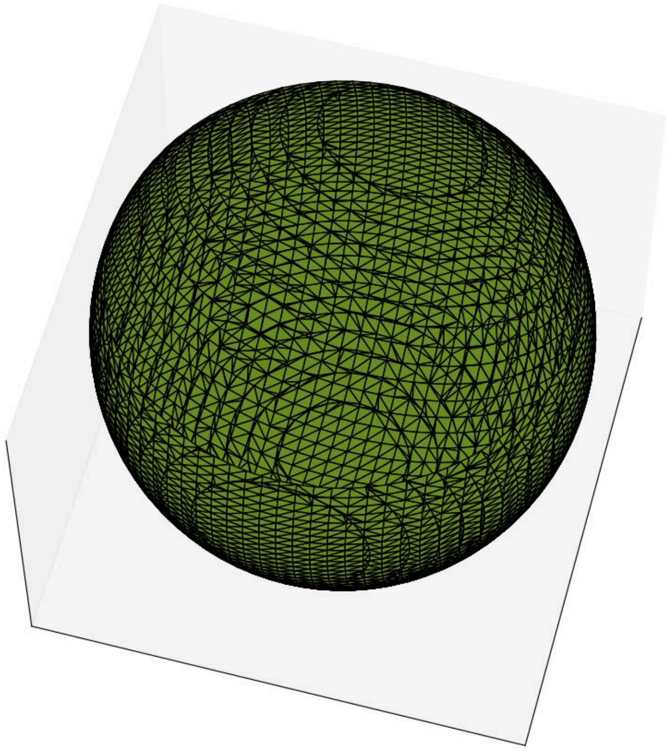

🎓 Implicit Surface Functions

Level-set idea: Represent a set $G(t)$ as an **isosurface of a scalar function** $\phi(x, t)$[1]:

- **State-space dimension does not matter conceptually**: the same ϕ machinery works in any n.
- Surfaces **automatically merge and separate** as the set evolves.
- **Geometric quantities** (normals, curvature, distance) are easy to compute from ϕ.

> Critical talk juncture: the reachable set is the zero sublevel set of a value function ϕ.

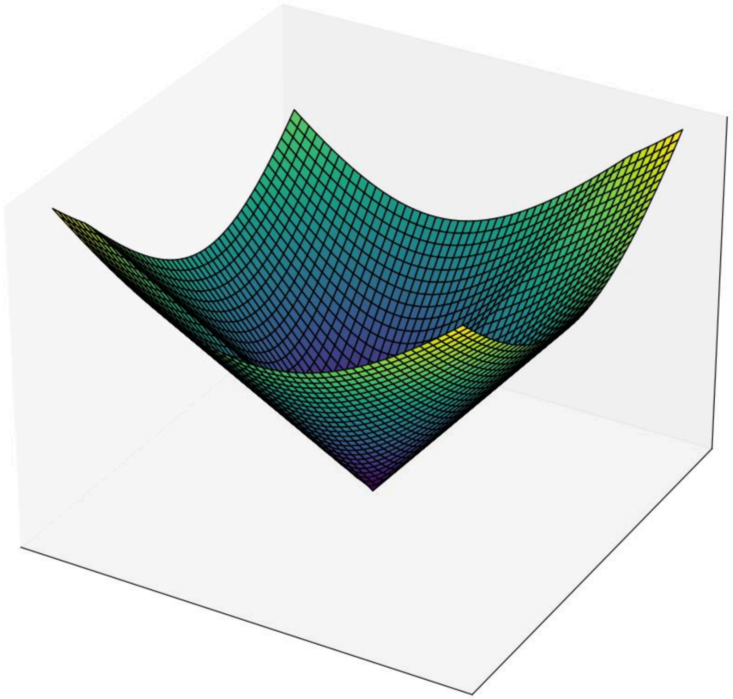

Inset: Set union of two spheres — LevelSetPy (L. Molu), ACM TOMS 51(2), 2025. · [1] Osher & Sethian

🎓 How to *Represent* the Set/Tube?

For continuous systems $\dot{x} = f(x)$, two families:

- **Lagrangian** (forward sets; restricted dynamics/shapes; overapproximation): HyTech, Checkmate, d/dt, ellipsoidal[1].
- **Eulerian** (backward sets; general dynamics incl. competitive inputs; **implicit** set representation).
  - **HJ-Gauss** belongs here.

[1] Kurzhanski

🎓 Canonical Example: Two Identical Vehicles

Classical collision avoidance:

- Collision if the vehicles come within **5 units** of each other.
- **Evader** picks turn rate $|a| \leq 1$ to *avoid*;
- **Pursuer** picks $|b| \leq 1$ to *cause* collision; fixed equal speeds $v_e = v_p = 5$.

(Mitchell 2004, Reach Sets and the HJ Equation)

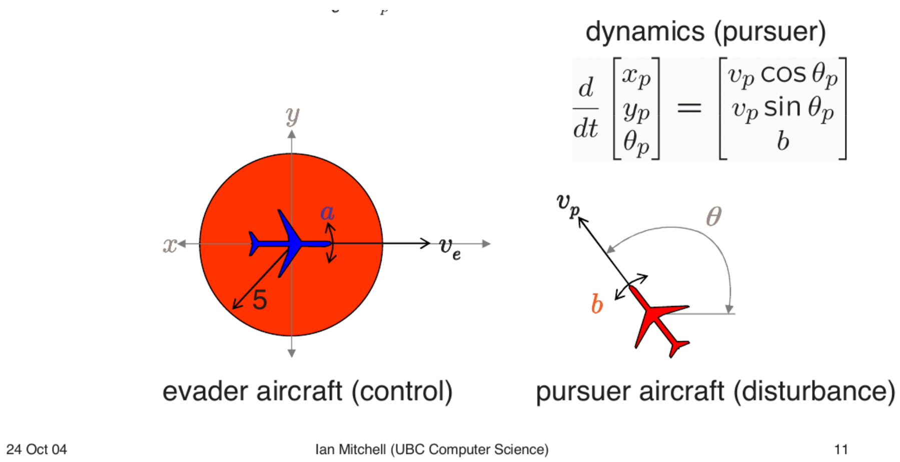

🎓 Canonical Example: Two Identical Vehicles

Classical collision avoidance:

- Work in **relative coordinates** with the evader fixed at the origin
- State is relative position (x, y) and relative heading ψ.

> NB: Same relative-coordinate pursuit-evasion (PE) game we solve with HJ-Gauss (Part 8); and the pairwise MAPF conflict of Part 9.

(Mitchell 2004, Reach Sets and the HJ Equation)

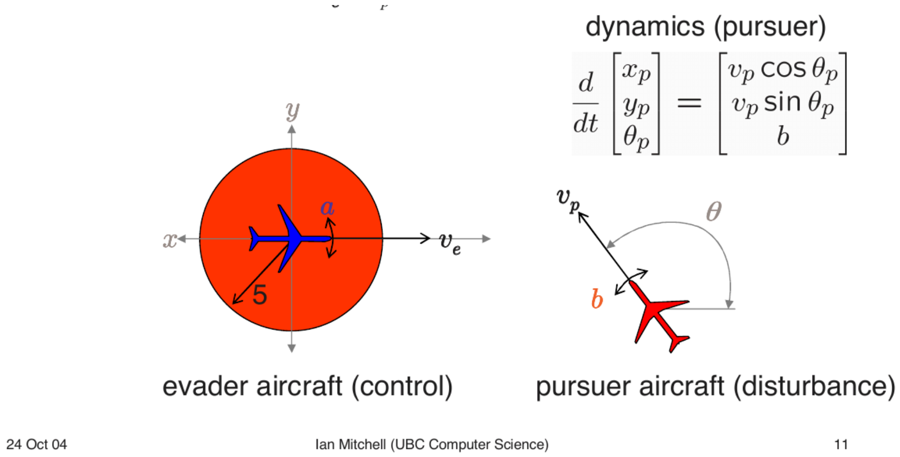

🎓 Evolve: The Time-Dependent HJ Equation

The set evolves by a (modified) Hamilton-Jacobi PDE:

- A **first-order hyperbolic PDE** whose solution can form **kinks** (discontinuous derivatives).
- The right weak solution is the **viscosity solution**[1].

(Mitchell 2004, Reach Sets and the HJ Equation); viscosity: Crandall-Evans-Lions; level sets: Osher-Sethian · Dubins BRT: LevelSetPy (L. Molu), ACM TOMS 51(2), 2025 · [1] Crandall, Evans, Lions

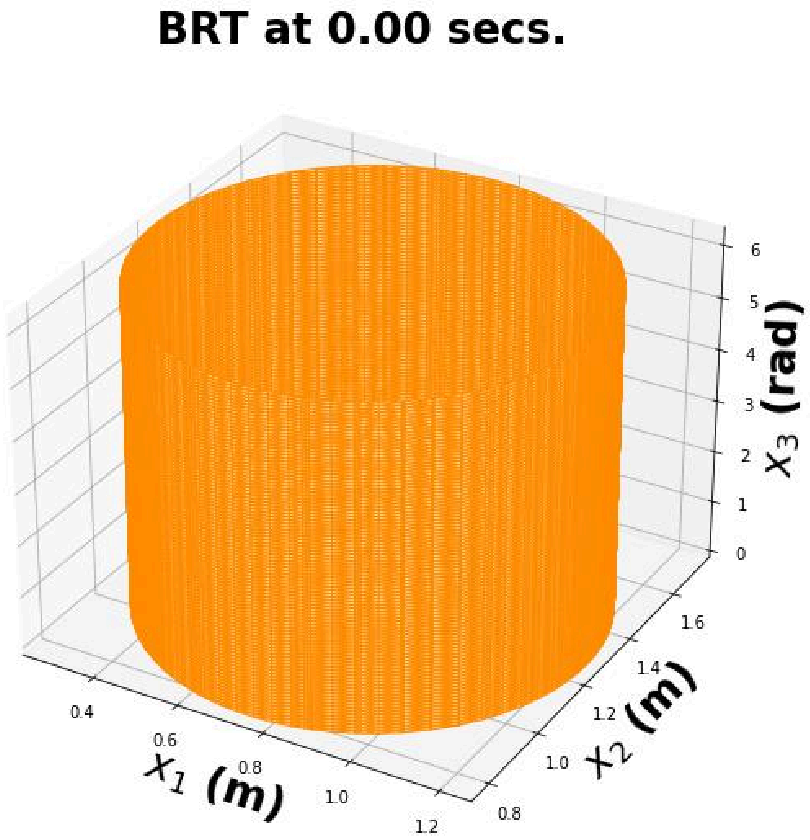

🎓 Evolve: The Time-Dependent HJ Equation

The set evolves by a (modified) Hamilton-Jacobi PDE:

- **Level-set methods** produce convergent numerical schemes[1]:
  - Non-oscillatory high-accuracy spatial derivatives;
  - A stable/consistent numerical Hamiltonian; and
  - Total variation-diminishing (TVD) high-order explicit time integration.

> This is the classical grid pipeline of Part 3. HJ-Gauss tackles this computational cost.

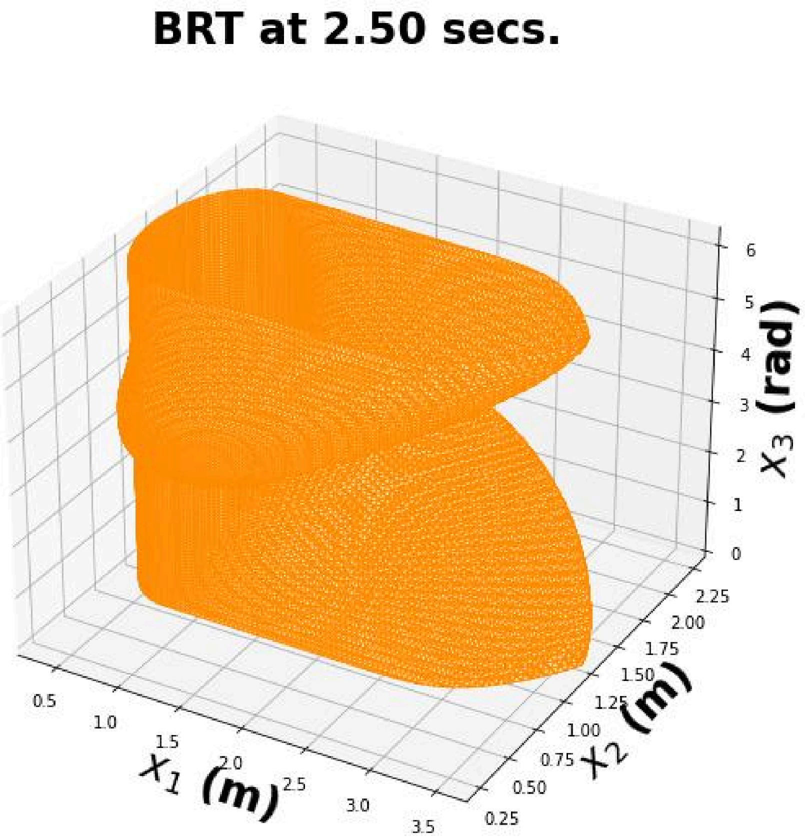

(Mitchell 2004, Reach Sets and the HJ Equation); viscosity: Crandall-Evans-Lions; level sets: Osher-Sethian · Dubins BRT: LevelSetPy (L. Molu), ACM TOMS 51(2), 2025 · [1] Osher, Sethian

🎓 The Game Value and the Optimal-Stopping Fix

- The **terminal-cost differential game**
  - Trajectories $\xi(\cdot; x, t, a, b)$;
  - **Value function** $\phi(x, t)$ is the viscosity solution of the HJ equation[1].

> This modified/augmented Hamiltonian is the $\min\{0, \cdot\}$ freeze term on our HJI-RCBRT slide.

[1] Evans & Souganidis, 1984

🎓 The Game Value and the Optimal-Stopping Fix

- To stop trajectories from passing *through* the target $G(0)$ (so the set is a **tube**, not just a set),
  - **Augment the disturbance input**;
  - The augmented HJ equation solves for the reachable set;
  - The augmented Hamiltonian is the modified $\min\{0, H\}$ Hamiltonian.

> This modified/augmented Hamiltonian is the $\min\{0, \cdot\}$ freeze term on our HJI-RCBRT slide.

🎓 Three Eulerian Approaches (All Equivalent)

The method sits among Eulerian formulations:

- **Static HJ**: Minimum time-to-reach[1]; (dis)continuous implicit representation; yields optimal-input information.
- **Viability kernels**: Set-valued analysis for very general dynamics[2]; discrete implicit representation; overapproximation guarantee.
- **Time-dependent HJ** (this method): Continuous solution, optimal-input information throughout the state space, high-order accurate.

> All three are **theoretically equivalent**; HJ-Gauss is a new *solver* for the time-dependent HJ formulation.

(Mitchell 2004, Reach Sets and the HJ Equation); Falcone/Sethian; Aubin/Saint-Pierre · [1] Falcone; Sethian · [2] Aubin; Saint-Pierre

🎓 Why It Matters: Two Applications

Reachable sets already drive real-world safety systems:

- **Softwalls for aircraft safety:** Filter evader's input so the pursuer never enters the reachable (unsafe) set — a certified safety filter (with E. Lee & A. Cataldo).
- **Collision alert for ATC:** Flag aircraft pairs whose flight plans intersect and whose relative state enters the collision region.
  - A one-hour Oakland-airspace sample: **1590 pairs, 25 detected conflicts, 2 false alerts**.

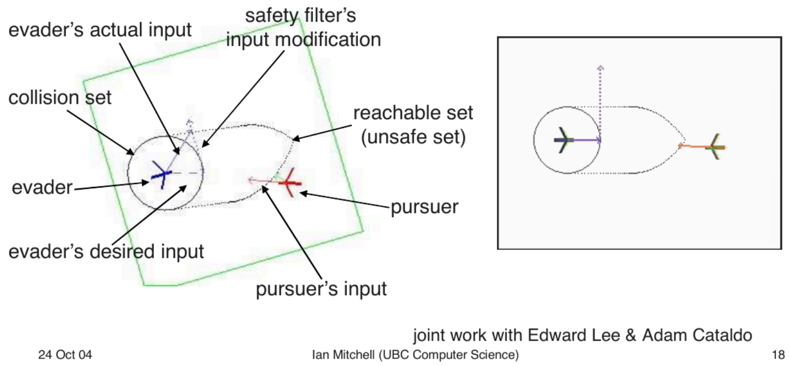

> These are the ancestors of the certified conflict predicate / shield we bring to warehouse MAPF in Part 9.

(Mitchell 2004, Reach Sets and the HJ Equation); Softwalls with E. Lee & A. Cataldo

🎓 Validation: Merz's Analytic Solution

- For **identical PE** dynamics, the reachable set admits an **analytic solution**[1].
- Merz placed the pursuer at the origin; the game is **not symmetric**.
- That analytic solution is used to **validate the numerical algorithm**[2] — the same discipline behind our LevelSetPy-vs-Monte-Carlo comparison in Part 8.

> Takeaway of the primer: reachability = represent implicitly, evolve in a HJ PDE game, solve for the viscosity solution.

> HJ-Gauss keeps this exactly and changes only *how* the PDE is solved.

(Mitchell 2004, Reach Sets and the HJ Equation); Merz (1972); Mitchell (2001) · [1] Merz, 1972 · [2] Mitchell, 2001

Target Set and Zero Level Set

- The **target set** at horizon T is the invariant set

$$\mathcal{L}_0(T) = \{x \in \mathbb{R}^n : \; v(0, x) \leq 0\},$$

robustly controlled over the **distance-to-target** cost $g(0, x)$.

- Numerically g is a **signed-distance function** $\ell(x)$ whose zero sublevel set is the target: negative inside, positive outside.
- The BRT is recovered as the **zero sublevel set** of the value function:

$$x(t) \in \mathcal{L}(\cdot) \iff v(t, x) \leq 0.$$

The Hamilton-Jacobi-Isaacs Value Function

The value function of the RCBRT is the **viscosity solution** of the variational HJ-Isaacs equation

$$v_t(t,x) + \min\{0,\ H(t;x,Dv)\} = 0, \qquad v(0,x) = g(0,x),$$

with the **game Hamiltonian**

$$H(t;x,p) = \max_u \min_w \langle p,\ f(t;x,u,w)\rangle.$$

- The $\min\{0,\cdot\}$ **freeze** term makes the set only *grow* (a tube, not a set) — states already captured stay captured.
- For reach-avoid, the variational inequality couples the growth term with the obstacle datum ℓ.

> This Hamiltonian is **positively 1-homogeneous in p, state-dependent, nonconvex, and sign-changing** across the barrier. Those four properties will rule out every convex-duality shortcut.

Reach vs Reach-Avoid; Sign & Time Conventions

- **Backward-reachability convention:** t is the **backward horizon** (time-to-go); the datum is posed at $t = 0$ and the tube grows over $(0, T]$.
- **Reach (capture) tube:** $v_t + \min\{0, H\} = 0$.
- **Reach-avoid tube (viscous):**

$$\min\left\{v_t^\delta + H^\delta - \tfrac{\delta}{2}\Delta v^\delta,\ \ g(t,x) - \ell(t,x)\right\} \leq 0.$$

- Physical time is $t_{\text{phys}} = T - t$; the datum is the terminal cost in physical time.

> These conventions matter for signs during implementation and for *which* set (reach vs avoid) a negative value certifies. We adopt the backward-reachability viscosity-solution convention throughout.

Why This Is the Right Safety Object

- **Worst-case, not average-case:** the RCBRT certifies safety against *all* admissible disturbances — the guarantee a safety case needs.
- **Geometric and set-valued, not trajectory-valued:** it characterizes *every* unsafe initial condition at once, not one rollout.
- **Composable:** the zero level set can be intersected, unioned, and propagated; it plugs into supervisory control and shielding.
- **Certificate-grade:** a signed value with an error bound yields a decision — SAFE / UNSAFE / UNDETERMINED (Part 7).

> The cost of this rigor is computational: solving the HJ(I) PDE. The rest of the talk is about paying that cost at scale.

Part 3

🧱 The Grid Pipeline: LevelSetPy

How Reachable Sets Are Computed Today — and Why It Is $O(M^n)$.

Molu. ACM TOMS 2025 · IEEE CDC 2024

TOMS: ACM Transactions on Mathematical Software · CDC: Conference on Decision and Control.

🧱 The Level-Set Idea[1]

- Represent the reachable set implicitly as the **zero sublevel set** of $v(t; x)$ stored on a Cartesian grid.
- Evolve the interface by integrating the HJ PDE on the grid:
  - Discretize space (upwinding),
  - Stabilize the Hamiltonian (Lax-Friedrichs),
  - March in time (TVD-RK).

[1] Osher-Sethian

🧱 The Level-Set Idea[1]

- **LevelSetPy** (our prior work) reimplements the 2004 MATLAB Level Set Toolbox in NumPy/CuPy, GPU-accelerated and interoperable with modern Python (PyTorch, SciPy, ROS).

MATLAB ToolboxLS (2004)	LevelSetPy (2024/25)
CPU-only, single-threaded	NumPy + **CuPy GPU**
Slow for modern problems	Fast, batched, portable
No modern-library plug-in	ROS/PyTorch/SciPy compatible

> LevelSetPy makes grid reachability *fast*. It does not change the *memory scaling* — the theme of Part 4.

[1] Osher-Sethian

🧱 Implicit Surfaces & Signed-Distance Initialization

- The target set is initialized as a **signed-distance function** $\ell(x)$: negative inside, positive outside, $|\nabla\ell| = 1$.
- Stored as an n-dimensional array over a Cartesian grid: M points per axis → M^n cells.
- Geometric primitives (spheres, cylinders, half-spaces) and boolean set operations (union/intersection/complement) are implemented as min/max on the level-set field.
- Example: a capture ball of radius r is $\ell(x) = \|x\| - r$; a cylinder ignores the periodic θ axis.

> The implicit representation is elegant and closed under set algebra — but it stores the value at **every** grid node.

🧱 Spatial Derivatives via Upwinding

- The co-state $p = \partial v / \partial x$ must be approximated from grid values with the correct **direction of information flow** (upwinding) to remain stable at shocks.
- **First-order upwinding:** one-sided differences chosen by the sign of the characteristic speed.
- Left/right approximations $D^{-}v,\ D^{+}v$ feed the numerical Hamiltonian; the choice prevents differencing across a discontinuity.

$$v_x(x,t) \approx \frac{\partial v(x,t)}{\partial x} \quad \text{(one-sided, direction by wind)}.$$

> Naive centered differences ring and go unstable at the barrier; upwinding is the minimal fix, refined next by ENO/WENO.

🧱 ENO: Essentially Non-Oscillatory Reconstruction

- **ENO** picks, among candidate stencils, the **smoothest** one to interpolate the derivative — avoiding stencils that straddle a shock.
- Orders implemented: **ENO2** (2nd), **ENO3** (3rd), via `upwind_first_eno2.py`, `upwind_first_eno3.py`.
- Higher order → sharper interface, lower numerical diffusion, at more stencil work per node.

> ENO chooses *one* smoothest stencil. WENO improves on this by blending stencils with adaptive weights.

🧱 WENO5: Weighted ENO Shock Capture

- **WENO5**[1] forms a **convex combination** of three candidate substencils rather than choosing one, achieving 5th-order accuracy in smooth regions and non-oscillatory capture at shocks.
- Substencils on the grid index i:

$$\{i-3,\ldots,i\},\quad \{i-2,\ldots,i+1\},\quad \{i-1,\ldots,i+3\},$$

combined with nonlinear weights that de-emphasize stencils crossing a discontinuity.

- Implemented in `upwind_first_weno5.py`.

> WENO5 is the workhorse for accurate reachable-set boundaries — and its per-node cost is one reason grid solves are expensive even before the memory wall.

[1] Liu, Osher, Chan 1994

🧱 The Lax-Friedrichs Numerical Hamiltonian

- The analytic $H(x,p)$ is replaced by a **monotone numerical Hamiltonian** $\hat{H}(x,p^-,p^+)$ using the Lax-Friedrichs flux:

$$\hat{H} = H\left(x, \frac{p^- + p^+}{2}\right) - \frac{1}{2}\alpha \cdot (p^+ - p^-),$$

with dissipation coefficient $\alpha = \max|\partial H/\partial p|$ over the relevant range (dimension-wise for global LF).

- Monotonicity guarantees convergence to the viscosity solution.

> The artificial dissipation α is a *numerical* cousin of the viscosity δ — both stabilize the barrier. HJ-Gauss will trade the grid's LF dissipation for the analytic δ.

🧱 Time Integration: TVD Runge-Kutta

Method of lines + **Total-Variation-Diminishing Runge-Kutta**[1], so the interface does not spuriously oscillate:

- **Forward Euler (1st):** $v^{n+1} = v^n + \Delta t\, L(v^n)$, $L = -\hat{H}$.
- **TVD-RK2:** Euler step to $v^{(1)}$, second Euler step, then convex average $v^{n+1} = \frac{1}{2}v^n + \frac{1}{2}v^{(2)}$.
- **TVD-RK3:** three stages with convex-combination weights $(1), (3/4, 1/4), (1/3, 2/3)$.

> TVD-RK preserves monotonicity of the spatial scheme in time. Each stage is a full grid sweep.

[1] Shu-Osher

🧱 The CFL Condition

- Explicit integration is stable only under a **Courant-Friedrichs-Lewy** step restriction:

$$\Delta t \;\le\; \frac{\mathrm{CFL}}{\sum_i \max\left|\partial H/\partial p_i\right|/\Delta x_i}, \qquad \mathrm{CFL} \in (0,1).$$

- Numerical information must not travel more than one grid cell per step.
- Finer grids ($\Delta x \downarrow$) force **smaller Δt** → more steps → compounding the cost.

> CFL couples spatial and temporal resolution: refining space to sharpen the barrier makes *both* the memory and the step count worse.

🧱 Package Anatomy & a Worked Example

Module	Role
`grids`, `initialconditions`	Cartesian grids, signed-distance shapes
`spatialderivative`	Upwind first, ENO2/3, WENO5
`explicitintegration`	Lax-Friedrichs Hamiltonians, TVD-RK, CFL
`dynamicalsystems`	Vehicle models (Dubins, rockets)
`visualization`	Isosurface / marching cubes rendering

- **Worked example:** the rockets-launch pursuit-evasion game; 2D (x, z) slices of the 3D relative-state BRT, evolved backward over $(0, T]$.
- Multi-agent verification: flocks/murmurations partitioned into per-flock games.

> A clean, tested, GPU-portable stack — the state of practice we now try to move beyond.

🧱 Grid Complexity: The Accounting

- **Memory:** $O(M^n)$ — store the value (and gradient) at every node.
- **Time per step:** $O(M^n)$ node updates × stencil width × RK stages, under a CFL-bounded step count.
- GPU acceleration cuts the *constant* and parallelizes node updates, but the **exponent n is untouched**.

$$n = 6,\ M = 100 \ \Rightarrow\ 10^{12}\ \text{cells}\ \approx\ 8\ \text{TB per double array.}$$

> This is the wall. Part 4 quantifies it and surveys who has tried to climb it.

Part 4

🧱 The Wall

Curse of dimensionality, and who has tried to climb it.

🧱 The Curse of Dimensionality, Quantified

Grid memory is $O(M^n)$ with M points per dimension:

State dim n	$M = 100$ cells	Feasibility (double array)
2	10^4	✅ trivial
3	10^6	✅ easy
4	10^8	⚠️ ~0.8 GB, heavy
5	10^{10}	❌ ~80 GB
6	10^{12}	❌ ~8 TB
45 (our multi-agent game)	10^{90}	❌ exceeds atoms in the observable universe

- Even a coarse $M = 101$ grid at $n = 45$ needs $101^{45} \approx 10^{90}$ cells.
- GPU acceleration lowers wall-clock, **not** the exponent.

> Reachability's most valuable regime — many interacting agents, rich dynamics — is where grids are impossible.

🧱 Attempt 1: PINN Reachability (DeepReach)

- **DeepReach** trains a neural network to minimize the HJ PDE residual directly (physics-informed loss), no reference grid.
- **Pro:**Trades grid storage for network weights; sidesteps $O(M^n)$ memory.
- **Con:** Scales only to moderate dimensiond (reported ~9-10D);
    - And **accuracy degrades** as n grows; training is a nonconvex optimization with no viscosity-solution guarantee.

> **Catch-22:** Learning-based solvers help, but do not deliver a certified, dimension-robust representation. **HJ-Gauss** keeps the viscosity-solution semantics.

🧱 Attempt 2: Convex-Duality Formulas (Hopf / Lax-Oleinik)

> HJ-Gauss trades their exactness for generality, at the quantified price of a linearization residual bound (Part 7).

- **Hopf** and **Lax-Oleinik** formulas[1] evaluate the value **pointwise** via convex optimization — grid-free at a point.
- **Limitation:** they require a **convex** (or state-independent) Hamiltonian.
- Reachability's $H(x,p) = \max_u \min_w \langle p, f \rangle$ is **state-dependent and nonconvex** → outside this class.

> It handles the nonconvex, state-dependent Hamiltonian head-on.

[1] Darbon-Osher 2016; Chow-Darbon-Osher-Yin 2017; Kirchner 2018

Attempts 3-4: Decomposition, Path Integral, Sampling

Family	Idea	Boundary
System decomposition[1]	Remove dimension by splitting self-contained subsystems	Only when coupling structure permits; HJ-Gauss is indifferent to coupling and *complements* it
Stochastic PDE / path integral[2]	Log-substitution linearizes the **stochastic** HJB under noise-control duality	Diffusion comes from *process noise*; ours is a **deterministic worst-case game**, δ an analysis parameter
Sample-based stochastic reachability[3]	Certify **probabilistic** reach-avoid	We certify **adversarial worst-case** reachability — a different, stronger guarantee

> **The open gap:** a grid-free, storage-light scheme for **nonconvex, state-dependent, adversarial** Hamiltonians. That is HJ-Gauss.

[1] Chen-Herbert · [2] Kappen; Theodorou · [3] Summers-Lygeros; Lesser-Oishi

🧱 Where HJ-Gauss Sits

- Keeps the **viscosity-solution** semantics (unlike PINN heuristics).
- Handles **nonconvex, state-dependent** H (unlike Hopf/Lax-Oleinik).
- **Indifferent to coupling structure** (complements decomposition).
- Certifies **adversarial worst-case** safety (unlike probabilistic sampling).
- Memory $O(N \cdot n)$, grid- and discretization-free.

> The rest is *how*: a Cole-Hopf transformation, a Feynman-Kac expectation, and a frozen-coefficient Picard iteration.

Part 5

🌊 HJ-Gauss Core Theory

Cole-Hopf Transformation → Linear Heat Equation

↓

→ Feynman-Kac Formula → Picard Iteration.

The Theoretical Roadmap of the Method

1. Start from the **viscous** HJ PDE (Part 1).
2. Apply a generalized **Cole-Hopf** transform $\omega = e^{-cv}$ → a **Linear heat equation**.
3. Solve the heat equation by its **Gaussian heat kernel** → a **Feynman-Kac expectation**.
4. Recover value (log-sum-exp) and gradient from that expectation.
5. Because c depends on the unknown Dv, **iterate**: freeze, solve, update (Picard) = **Algorithm 1**.
6. Analyze exactness (quadratic case) vs the **quasi-linearization residual** (general case).

> Each arrow is a theorem or proposition in the paper; we walk them one by one.

The Transformation, and the Closed-Form/Approximate Split

For a general H, define the spatially-varying coefficient

$$c(t;x) = \frac{2}{\delta} \cdot \frac{H^\delta}{|Dv^\delta|^2}, \qquad H^\delta := H(t;x,Dv^\delta),$$

and set $\omega^\delta := \exp(-c\,v^\delta)$.

- **Quadratic case** $H = \frac{1}{2}|p|^2$: $c = 1/\delta$ constant, ω^δ solves the **homogeneous heat equation** with **zero residual** — a genuine Cole-Hopf identity.
- **General** H: the transform induces a residual $R = R_{\text{alg}} + R_{\text{der}}$;
  - c's choice eliminates the **algebraic** part R_{alg}, leaving the **derivative** part R_{der}.

> No freezing of c's *values* removes its *derivatives*. Hence for nonlinear H this is a **quasi-linearization**, not an identity — and the leftover R_{der} is the residual we will bound.

Picard Quasi-Linearization: The Surrogate View

- At iteration k, **freeze $c^{(k)}$** at the current iterate and solve the linear heat equation **in closed form**.
- Equivalently: replace the true Hamiltonian by the **locally-matched quadratic surrogate**

$$\tilde{H}^{(k)}(p) = \tfrac{\delta}{2}\, c^{(k)}\, |p|^2,$$

solve the resulting viscous HJ equation in closed form, obtain $v^{(k+1)}$, update $Dv^{(k+1)}$ and $c^{(k+1)}$.

- **The iteration's limit is the fixed point of the surrogate solve map** — equal to the viscous solution *only* when $R_{\mathrm{der}} \equiv 0$ (the quadratic case).

> "Successive quadratic matching": each step is a locally closed-form quadratic-Hamiltonian solve, refined by re-estimating the co-state.

Reduction to the Heat Equation (Proposition)

With $c^{(k)}$ frozen, ω^δ solves the heat initial-value problem

$$\omega^\delta_t - \tfrac{\delta}{2}\Delta\omega^\delta = 0 \;\text{ in } \mathbb{R}^n \times (0,T], \qquad \omega^\delta(0,x) = \exp(-c\, g(x)).$$

- When $H = \frac{1}{2}|p|^2,\ c = 1/\delta$: **closed-form, no residual**.
- For general H: discards the derivative residual (Lemma, appendix) — the quasi-linearization.

> A nonlinear, nonconvex, state-dependent HJ PDE has become **the heat equation** — the most classical linear parabolic PDE, with an explicit Gaussian solution.

The Gaussian Heat Kernel & Feynman-Kac

The heat IVP has the unique bounded Green's-convolution solution

$$\omega^\delta(t,x) = \frac{1}{(\sqrt{2\pi\delta t})^n} \int_{\mathbb{R}^n} e^{-\frac{|x-y|^2}{2\delta t}}\, e^{-c\,g(y)}\, dy,$$

which, by **Feynman-Kac**, is a **Gaussian expectation**:

$$\omega^\delta(t,x) = \mathbb{E}_{y\sim\mathcal{N}(x,\,\delta t I_n)}\left[e^{-c\,g(y)}\right].$$

- The free-space kernel integrates to one over $\mathbb{R}^n$ (and no proper subset) — every estimator is posed on all of $\mathbb{R}^n$.
- Sampling $y \sim \mathcal{N}(x, \delta t I_n)$ and averaging $e^{-cg(y)}$ is an **unbiased** estimator of ω^δ.

> The solution is a **Gaussian roll-out average of the terminal cost**. This is the entire computational payload — no grid, no marching.

Recovering the Value (Lemma)

Invert the transform:

$$v^{\delta}(t,x) = -\frac{1}{c^{(k)}} \log \mathbb{E}_{y\sim\mathcal{N}(x,\delta t I_n)}\left[e^{-c^{(k)} g(y)}\right].$$

- A **log-sum-exp** of Gaussian-sampled terminal costs.
- Numerically evaluated in a **log-domain-stable** form (log-mean-exp) to avoid overflow/underflow.
- M arbitrary evaluation states $x_1, \ldots, x_M$ — laid on a grid or scattered — each with its own fresh N samples.

> The value at a query point is a scalar reduction over N samples. Embarrassingly parallel across both M states and N samples.

Recovering the Gradient (Corollary)

The spatial gradient (co-state) has a closed Gaussian-expectation form:

$$Dv^{\delta} = \frac{1}{t\,\delta\,c^{(k)}}\left(x - \frac{\mathbb{E}_{y\sim\mathcal{N}(x,\delta t I_n)}\left[y\,e^{-c^{(k)}g(y)}\right]}{\mathbb{E}_{y\sim\mathcal{N}(x,\delta t I_n)}\left[e^{-c^{(k)}g(y)}\right]}\right).$$

- A **weighted-mean shift**: the gradient points from x toward the exponentially-weighted centroid of the samples.
- No finite differencing, no stored field — the co-state is a byproduct of the same samples.

> This gradient is (up to constants) a **score function** $\nabla \log \omega$. Hold that: it is the entire bridge to diffusion in Part 10.

Admissible Data & Unbiasedness (Recap as a Guarantee)

- Datum $\omega^\delta(0,\cdot) = e^{-cg}$ is continuous, strictly positive, bounded above by $e^{-cg_{\min}}$, decaying at infinity.
- $\Rightarrow$ the heat solution is the **unique bounded** one; the integral converges absolutely; the Gaussian expectation is **genuine and unbiased**.
- Only $g \geq g_{\min}$ is required (bounded target); no upper bound on g.

> The estimator drawing $y \sim \mathcal{N}(x, \delta t I_n)$ over all of $\mathbb{R}^n$ is **unbiased for the quantity inside the logarithm** — the foundation for the concentration bound of Part 7.

Sign and the Removable Zero of the Coefficient

- $c \sim C_H/(\delta|Dv^\delta|)$: it **grows without bound** in flat regions and **vanishes and flips sign** where optimal dynamics run tangent to the level set (the barrier).
- The zero of c is a **removable** singularity of the estimator: as $c \to 0$,

$$-\frac{1}{c}\log \mathbb{E}[e^{-cg}] \;\to\; \mathbb{E}[g],$$

i.e. the log-sum-exp gracefully degenerates to the **Gaussian mean** of the terminal data — the correct pure-diffusion limit ($H \to 0$ reduces the PDE to the heat equation).

- In implementation: evaluate in a `log1p`-stable form and **clip** $|c|$ to $[c_{\min}, c_{\max}]$.

> The coefficient's pathologies are analytically understood and numerically tamed — clipping is itself a bounded, priced perturbation (next slide).

Coefficient Regularization (Lemma)

Run Algorithm 1 with the **regularized coefficient**

$$c_\eta(t;x) = \frac{2}{\delta} \cdot \frac{H^\delta}{|Dv^\delta|^2 + \eta},$$

equivalent to running it unregularized for the **perturbed Hamiltonian** $H_\eta = H\,|Dv^\delta|^2/(|Dv^\delta|^2 + \eta)$, which satisfies a **uniform** bound

$$\|H_\eta - H\|_\infty \le \frac{C_H\sqrt{\eta}}{2},$$

so the induced value-function perturbation is at most $TC_H\sqrt{\eta}/2$.

> Regularization cures the flat-interior blow-up at a **quantified, uniform** price — no hidden instability.

Algorithm 1: Quasi-Linearization (Cole-Hopf)

$$\text{Fix } \varepsilon > 0, \qquad v^{(0)}(t,x) = g(x), \qquad c^{(0)} = \frac{2\,H(t,x,Dg)}{\delta\,|Dg|^2}.$$

$$\textbf{for } \; k = 0, 1, 2, \ldots:$$

$$(1) \text{ freeze } c^{(k)} \text{ at the current iterate;}$$

$$(2) \text{ solve } \; \omega_t = \tfrac{\delta}{2}\Delta\omega, \;\; \omega^{(k)}(0,x) = e^{-c^{(k)} g(x)};$$

$$\Rightarrow \;\; \omega^{(k+1)}(t,x) = \mathbb{E}_{y\sim\mathcal{N}(x,\delta t I)}\big[e^{-c^{(k)} g(y)}\big] \;\; \text{(Monte-Carlo);}$$

$$(3) \text{ recover } \; v^{(k+1)} = -\tfrac{1}{c^{(k)}} \log \omega^{(k+1)};$$

$$(4) \text{ update } Dv^{(k+1)}, \;\; c^{(k+1)} = \frac{2\,H(t,x,Dv^{(k+1)})}{\delta\,|Dv^{(k+1)}|^2} \;\; \text{clip to } [c_{\min}, c_{\max}];$$

$$(5) \text{ stop when } \; \|v^{(k+1)} - v^{(k)}\|/\|v^{(k)}\| < \varepsilon.$$

- Steps (2)-(4) are all **Gaussian-expectation reductions** over N samples.
- Convergence typically in ≤ 20 iterations (empirically 12-15).

> Every line is grid-free. The only state carried between iterations is the coefficient field $c^{(k)}$ at the M evaluation states.

Evaluation States vs Monte-Carlo Samples (Remark)

- N = i.i.d. Gaussian draws $y_1, \ldots, y_N \sim \mathcal{N}(x, \delta t I_n)$ used **independently at each** evaluation state x to form the estimators.
- Resampled **fresh** at every evaluation state and every Picard iteration.
- M = the evaluation states $x_1, \ldots, x_M$ where v is queried — carry **no randomness**, may be a uniform grid or scattered arbitrarily.
- Total randomness per iteration: $M \times N$ **draws**.
- The zero level set is recovered by evaluating v^δ at the M states and isocontouring at level zero (marching cubes) — a deterministic post-process consuming **no further samples**.

> The **solve is grid-free**; the grids that appear in results are *evaluation windows* for visualization and error measurement, not sampling constraints.

Memory: $O(N \cdot n)$ vs $O(M^n)$

	Grid level sets	HJ-Gauss
Representation	Stored field on M^n grid	N Gaussian samples per query, n-vectors
Memory	$O(M^n)$	$O(N \cdot n)$
Discretization	Cartesian grid + marching cubes to *solve*	None (grid-free solve)
Query states	Tied to grid	Arbitrary / scattered
Parallelism	Grid array ops	Over M states **and** N samples

- Example: $N = 14{,}000,\ n = 3$ → ≈ 0.6 MB/iteration; $n = 45$ → ≈ 7.2 MB/iteration (vs 10^{90} grid cells).

> Memory now scales with **sample budget and dimension**, not with a grid raised to the dimension. This is the whole contribution in one line.

Part 6

🎯 Importance Sampling & Variance Control

Making the Gaussian estimator work in high dimensions.

🎯 The Weight-Degeneracy Problem

- The estimators are a **ratio of exponential-weight expectations**, e.g. the gradient's numerator/denominator both carry e^{-cg}.
- In high dimensions (or small δ), $c\,g$ is large over the kernel support, so the denominator $\mathbb{E}[e^{-cg}]$ is carried by a **rare event**.
- The weights collapse onto a few samples → the ratio's **variance explodes**; the effective sample size crashes.

> Naive Gaussian sampling is unbiased but can be catastrophically high-variance right where we need it (high n, small δ). We fix it with importance sampling.

🎯 Tilted Proposal & Density-Ratio Reweighting

- Replace $y \sim \mathcal{N}(x, \sigma^2 I_n)$ ($\sigma^2 = \delta t$) by a **shifted** proposal $q_\theta = \mathcal{N}(x + \theta, \sigma^2 I_n)$.
- Reweight by the **density ratio**

$$w_\theta(y) = \exp\left(\frac{|\theta|^2 - 2\langle y - x, \theta\rangle}{2\sigma^2}\right),$$

which leaves **every expectation unbiased**.

> We move the samples to where the integrand has mass, then correct via the ratio. Bias is untouched; variance can collapse by orders of magnitude.

🎯 The Zero-Variance Shift Is One Gradient Step

- The zero-variance proposal is proportional to the integrand $\varphi_x(y)\, e^{-cg(y)}$ itself.
- Its first-order **Laplace / Gaussian** approximation gives the shift

$$\theta^\star = -\sigma^2\, c^{(k)}\, Dv^{(k)}(t,x).$$

- That is, samples are pushed **one preconditioned gradient step** along the descent direction of the running value iterate.

> **The previous Picard iterate hands the sampler its drift for free.** Reachability and importance sampling become the *same* computation — the value gradient is the optimal sampling direction.

🎯 Effective Sample Size as a Self-Diagnostic

- Monitor the **effective sample size** of the self-normalized weights $\tilde{w}_i = w_\theta(y_i)e^{-cg(y_i)}$:

$$\mathrm{ESS} = \frac{\left(\sum_i \tilde{w}_i\right)^2}{\sum_i \tilde{w}_i^2} \in [1, N].$$

- $\mathrm{ESS} \approx N$: weights well-spread → estimate certified.
- $\mathrm{ESS} \to 1$: **weight degeneracy** → flag, increase N, raise δ, or re-tilt.

> ESS is a free, per-query health check: it tells you *when* to trust the estimate and *why* it failed when it does.

Part 7

📐 Guarantees

Concentration · contraction · residual · total error · certificate · robustness.

📐 Four Error Sources, One Budget

The distance from the computed field $\hat{v}^{K,N,\delta}$ to the true inviscid viscosity solution v decomposes into four independently-controlled sources:

Source	Controlled by	Scaling
Iteration (Picard truncation at K)	More iterations	$C_1 \rho^K$
Monte-Carlo (finite N)	More samples	$C_2 N^{-1/2} \sqrt{\log(1/\delta_p)}$
Quasi-linearization residual $\mathcal{E}_{\mathrm{ql}}$	Surrogate fidelity (not effort)	Floor
Viscosity (finite δ)	Smaller δ	$C_3 \sqrt{\delta}$

> Three of four shrink with computational effort; the **residual is a property of the surrogate** and sets the floor. We now bound each.

📐 Finite-Sample Concentration (Theorem)

Fix phase (t, x) and frozen $c > 0$; assume $g_{\min} \le g \le g_{\max}$ on the sampling support. With $Z = e^{-cg(\zeta)}$, $\mu = \mathbb{E}[Z]$, $v_c = -\frac{1}{c}\log\mu$, $\alpha = e^{-cg_{\max}}$, $\beta = e^{-cg_{\min}}$, and $\hat{v}_{c,N} = -\frac{1}{c}\log\bar{Z}_N$:

$$\mathbb{P}(|\hat{v}_{c,N} - v_c| \ge \varepsilon) \;\le\; 2\exp\left(-\frac{2N\mu^2(1-e^{-c\varepsilon})^2}{(\beta-\alpha)^2}\right).$$

- Bounded weights $\alpha \le Z_i \le \beta$ ⇒ Hoeffding.
- Rate is the standard $O(N^{-1/2})$, **independent of state dimension n** — the crux of the scalability claim.

> Dimension enters the *cost per sample*, not the *number of samples* for a target accuracy. That is how we beat $O(M^n)$.

📐 Explicit Sample Size, and Its Worst Case (Corollary + Remark)

- Since $\mu \geq \alpha$, it suffices to take

$$N \;\geq\; \frac{(\beta-\alpha)^2}{2\alpha^2(1-e^{-c\varepsilon})^2}\log\frac{2}{\alpha}$$

to guarantee error $\geq \varepsilon$ with probability $\leq \alpha$.

- **Worst-case caveat:** with $c = 1/\delta$, $\beta/\alpha = e^{(g_{\max}-g_{\min})/\delta}$, so this bound grows like $e^{2(g_{\max}-g_{\min})/\delta}$ — **exponential in $1/\delta$**, while viscosity error is only $O(\sqrt{\delta})$.

> The accuracy gain from shrinking δ and the sample cost pull **in opposite directions**. This Hoeffding bound is loose; the next slide tightens it, and experiments sit far below it.

📐 Tightening: Bernstein & Jensen

- **Bernstein:** when $\mathrm{Var}(Z) \ll (\beta - \alpha)^2/4$, a variance-aware tail bound gives strictly tighter concentration than Hoeffding.
- **Jensen:** the loose lower bound $\mu \geq \alpha = e^{-cg_{\max}}$ can be replaced by $\mu \geq e^{-c\,\mathbb{E}[g(\zeta)]}$, substantially reducing the required N.
- **Importance sampling** (Part 6) attacks the same variance directly.

> The pessimistic $e^{1/\delta}$ is a worst-case artifact of Hoeffding + crude μ bound. In practice $N \in [14\mathrm{k}, 20\mathrm{k}]$ suffices at $\delta \in [0.08, 0.1]$.

📐 The Iteration Operator (Contraction Setup)

- Fix evaluation states $x_1, \dots, x_M$ and time t; let $\mathcal{G}$ be a stable gradient-reconstruction operator, $p_m(v) = (\mathcal{G}v)_m$.
- Coefficient-update map: $(\Gamma(v))_m = 2H(t, x_m, p_m(v))/(\delta|p_m(v)|^2)$.
- Frozen-coefficient heat-kernel map:

$$(\Phi(c))_m = -\frac{1}{c_m} \log \mathbb{E}_{\zeta\sim\mathcal{N}(x_m,\delta t I_n)}\left[e^{-c_m g(\zeta)}\right].$$

- Algorithm 1 is the iteration $v^{(k+1)} = \Lambda(v^{(k)})$, $\Lambda = \Phi \circ \Gamma$.

> The whole method is a fixed-point iteration of a composed map on $\mathbb{R}^M$ with the sup-norm. Contraction $\Rightarrow$ convergence.

📐 Assumptions for Contraction (Assumption A)

On a closed admissible set $\mathcal{A}$ (sup-norm), assume:

1. $|g| \le G$;
2. non-degenerate gradient & bounded coefficient: $m_0 \le |p_m| \le P_*$, $c_{\min} \le (\Gamma v)_m \le c_{\max}$;
3. Hamiltonian Lipschitz in co-state: $|H| \le H_*$, $|H(\cdot, p) - H(\cdot, q)| \le L_H |p - q|$;
4. reconstruction Lipschitz: $\|\mathcal{G}v - \mathcal{G}w\|_\infty \le L_D \|v - w\|_\infty$;
5. invariance + contraction constant

$$q = \frac{2G}{c_{\min}} \cdot \frac{2L_D}{\delta} \left(\frac{L_H}{m_0^2} + \frac{2H_* P_*}{m_0^4} \right) < 1.$$

> Non-degeneracy (item 2) holds on the **tube band** $\{|v^\delta| \le \eta\}$ where the gradient is bounded away from zero — where the barrier lives. Outside, use the regularized coefficient.

📐 Contraction Convergence (Theorem)

Λ is a **contraction** on $\mathcal{A} \Rightarrow$ unique fixed point $v^\star$, and for any $v^{(0)} \in \mathcal{A}$:

$$\|v^{(k+1)} - v^\star\|_\infty \le q\,\|v^{(k)} - v^\star\|_\infty \le q^{k+1}\|v^{(0)} - v^\star\|_\infty,$$

with the **a posteriori** estimate

$$\|v^{(k)} - v^\star\|_\infty \le \frac{q}{1-q}\,\|v^{(k)} - v^{(k-1)}\|_\infty.$$

- Iteration count for tolerance ε: $K = O(\log(1/\varepsilon))$ — **geometric** convergence.

> The residual you *watch* (successive-iterate change) bounds the error you *cannot see* (distance to $v^\star$). That is the a posteriori estimate — a runtime stopping certificate.

Scope of the Contraction (Remark)

- The theorem is about the **frozen-coefficient numerical map**, not the original nonlinear PDE.
- The fixed point $v^\star$ solves the viscous HJ equation with H replaced by its **quadratic surrogate at $v^\star$**.
- $v^\star = v^\delta$ iff $H = \frac{1}{2}|p|^2$ (then $c \equiv 1/\delta, R_{\text{der}} \equiv 0$).
- For general H, the two differ by the **quasi-linearization residual** $\mathcal{E}_{\text{ql}} = \|v^\star - v^\delta\|_\infty$.

> We do **not** claim unconditional global convergence to the true HJ solution. We claim geometric convergence to a surrogate fixed point, plus a **bound on the gap** — next.

📐 The Quasi-Linearization Residual (Theorem, via Duhamel)

With converged coefficient $c^\star$, coefficient-variation bound L_c, value bound G_v:

$$\mathcal{E}_{\mathrm{ql}} = \|v^\star - v^\delta\|_\infty \;\le\; \frac{T}{c_{\min}}\, e^{2c_{\max}G_v}\,\big(\bar{R}_{\mathrm{alg}} + \bar{R}_{\mathrm{der}}\big),$$

- $\bar{R}_{\mathrm{alg}} \le c_{\max}(L_H + 2H_* P_*/m_0^2)\,\|Dv^\delta - Dv^\star\|_\infty$ — **contracts as the surrogate gradient tracks the true one**.
- $\bar{R}_{\mathrm{der}} \le L_c G_v(1 + \frac{\delta}{2}) + \frac{\delta}{2} L_c^2 G_v^2 + \delta(1 + c_{\max}G_v)L_c P_*$ — governed by **coefficient variation L_c**.

Proof idea: $\tilde{\omega} = e^{-c^\star v^\delta}$ solves the heat equation with a source ωB (Lemma); Duhamel + heat-semigroup L^∞-contraction bounds $\|\tilde{\omega} - \omega^\star\|$; mean-value theorem for $\log$ converts back to v.

> The bound **vanishes in the quadratic case** ($L_c = 0, Dv^\star = Dv^\delta$) and is largest where $H/|Dv|^2$ turns over sharply — the usable-part boundary.

📐 Reading the Residual

- **Vanishes** when $H = \frac{1}{2}|p|^2$: recovers the closed-form Cole-Hopf.
- **Governed by L_c**, the variation rate of the converged coefficient — largest near the barrier where the Hamiltonian-to-gradient ratio shocks.
- **Algebraic part** $\propto \|Dv^\delta - Dv^\star\|$: the residual contracts as the Picard iteration refines the co-state.
- Certifies smallness where $c^\star$ is slowly varying; offers **no reprieve** where it is not.

> This is why experimental errors concentrate at the zero-level-set boundary — the theory *predicts* the location of the worst error.

📐 The Total Error Bound (Theorem) & Bias-Variance

Chaining all four sources by the triangle inequality:

$$\|\hat{v}^{K,N,\delta} - v\|_\infty \;\le\; C_1\rho^K + \frac{C_2}{\sqrt{N}}\sqrt{\log(1/\delta_p)} + \mathcal{E}_{\mathrm{ql}} + C_3\sqrt{\delta}.$$

- **Bias-variance tradeoff in δ:** viscosity bias $\downarrow$ as $\delta\downarrow$, but MC variance $\uparrow$.
- Balancing the two nontrivial δ-dependent terms yields the optimal

$$\delta \sim N^{-1/3} \;\Rightarrow\; \text{overall rate } O(N^{-1/6}),$$

slower than plain MC $O(N^{-1/2})$ but **dimension-robust and scalable**.

> A single decomposition tells you how to spend budget: iterate to kill ρ^K, sample to kill $N^{-1/2}$, choose $\delta \sim N^{-1/3}$, and accept the residual floor.

📐 The Conservative Safety Certificate (Corollary)

Let E be the total error budget. Declare state x:

- **SAFE** only if $\hat{v}^{K,N,\delta}(x) > E$;
- **UNSAFE** only if $\hat{v}^{K,N,\delta}(x) < -E$;
- **UNDETERMINED** otherwise ($|\hat{v}| \leq E$).

> With probability $\geq 1 - \delta_p$: **no unsafe state is certified safe** and **no safe state is certified unsafe**; all classification error is confined to a declared band of width $2E$ about the boundary.

- The certificate **errs on refusal, never on admission**.
- This is the accuracy quotation: **worst-case sign-correctness with an explicit abstention band**, not an L^2 average that flatters the interior.

Robustness to Model Uncertainty

- The scheme is **stable under small perturbations** of the Hamiltonian and terminal cost (robustness theorems, appendix): perturb H by ΔH in sup-norm ⇒ value perturbed by $\leq T\|\Delta H\|_\infty$ (Duhamel/comparison).
- Consequence: perfectly known dynamics and terminal costs are **not required** — real-world models with bounded error still yield certified-with-margin sets.
- The coefficient-clipping and regularization perturbations are of this priced form.

> The method degrades **gracefully and quantifiably** under model error — a prerequisite for deployment on real robots with imperfect models.

Part 8

🧪 Experiments (from the Paper)

Rockets, Dubins, a 45D game, and 10^5 birds.

🧪 Experimental Setup & Statistics BLUF - (1/2)

- **Hardware:** single CPU (Intel i7-14700K, 20 cores, 31 GiB RAM, Ubuntu 22.04); JAX on CPU backend

— Consistent with the memory-frugality claim.

- **Replication:** Each experiment re-solved with **30 independent Monte-Carlo seeds**;
    - Evaluation points and the LevelSetPy reference held fixed - only sampler randomness varies. Tables report mean ± 1 s.d.

> Figures show one representative seed for clarity; tables report full 30-seed statistics. Multiplicity-controlled reporting throughout.

🧪 Experimental Setup & Statistics BLUF - (2/2)

- **Significance:** Three families of **Holm-Bonferroni-corrected** tests at $\alpha = 0.05$:
  - (a) paired Wilcoxon of 30-seed-averaged MC field vs grid reference;
  - (b) one-sided t-test that per-seed L^2_{rel} lies below the Crandall-Lions bound $\sqrt{\delta}$;
  - (c) cross-condition Mann-Whitney (Rockets vs Dubins; speed regimes).

> Figures show one representative seed for clarity; tables report full 30-seed statistics. Multiplicity-controlled reporting throughout.

🧪 Benchmark 1: Two-Vehicle Pursuit-Evasion Games

- **Rockets launch game**[1]: two identical rockets — pursuer P, evader E — on the x-z plane, thrusts (u_p, u_e), relative orientation $\theta = u_p - u_e$. Capture when $\|PE\| < r$.
- **Dubins two-car game** (Merz): relative (x_1, x_2, θ), symmetric turn-rate bound.
- Both are **3D relative-state** games; the BRT is a 3D tube, visualized as 2D (x, z) slices at fixed θ.
- Target: ℓ_2-ball of capture radius $r = 1.5$; horizon $(0, 1]$; $\delta = 0.08$; $N = 14{,}000$ (rockets) / $20{,}000$ (Dubins) samples per iteration.

> These are the canonical HJ-Isaacs benchmarks — and the Dubins game is the pairwise MAPF conflict of Part 9.

[1] Dreyfus 1966

🧪 The Two-Rockets Problem (Schematic)

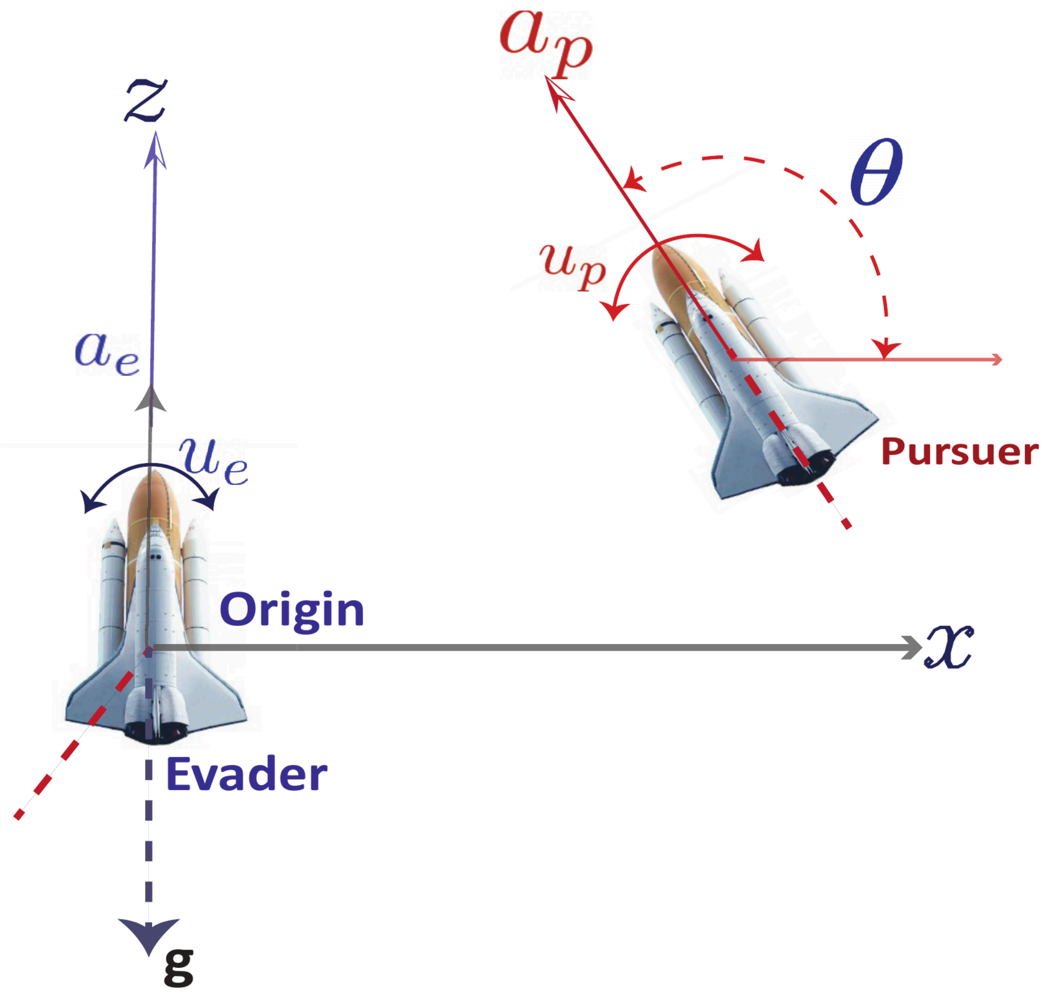

Relative geometry: evader E fixed at the origin (accel. a_e, control u_e, gravity g); pursuer P at relative orientation $\theta = u_p - u_e$ on the (x, z) plane. — HJ-Gauss (Molu et al., 2026).

🧪 The Dubins Air3D Problem (Schematic)

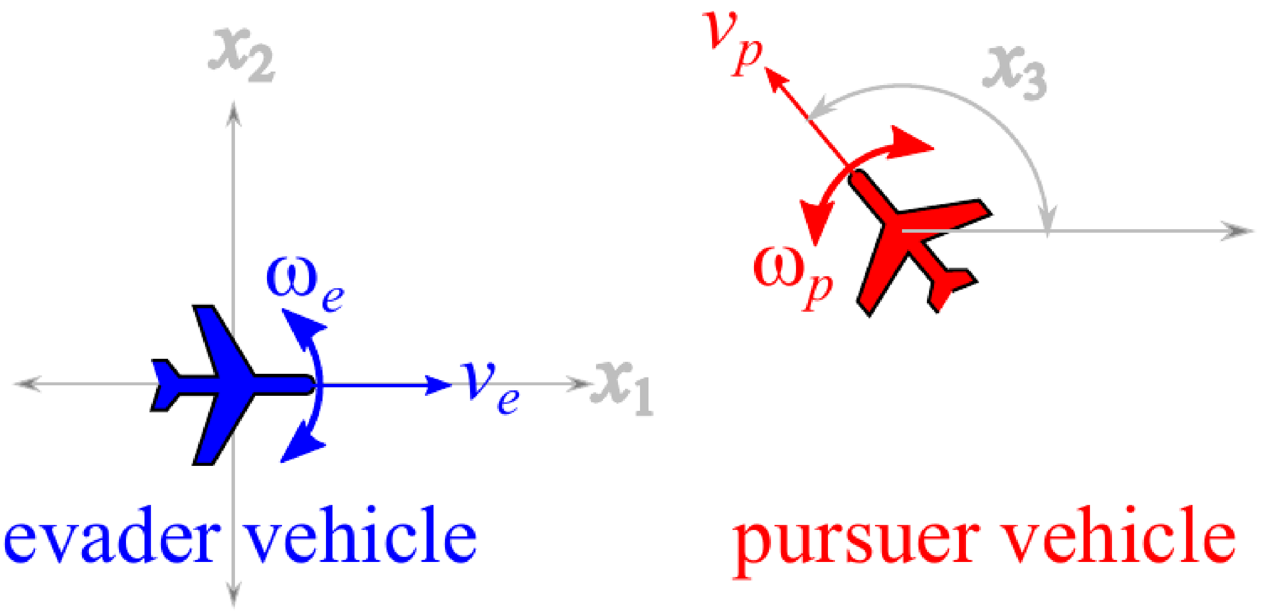

Air3D relative coordinates with the evader fixed at the origin: relative position (x_1, x_2) and relative heading ψ; turn-rate-bounded pursuer vs evader. — LevelSetPy (Molu, ACM TOMS 2025 / IEEE CDC 2024).

🧪 Rockets Pursuit-Evasion BRT

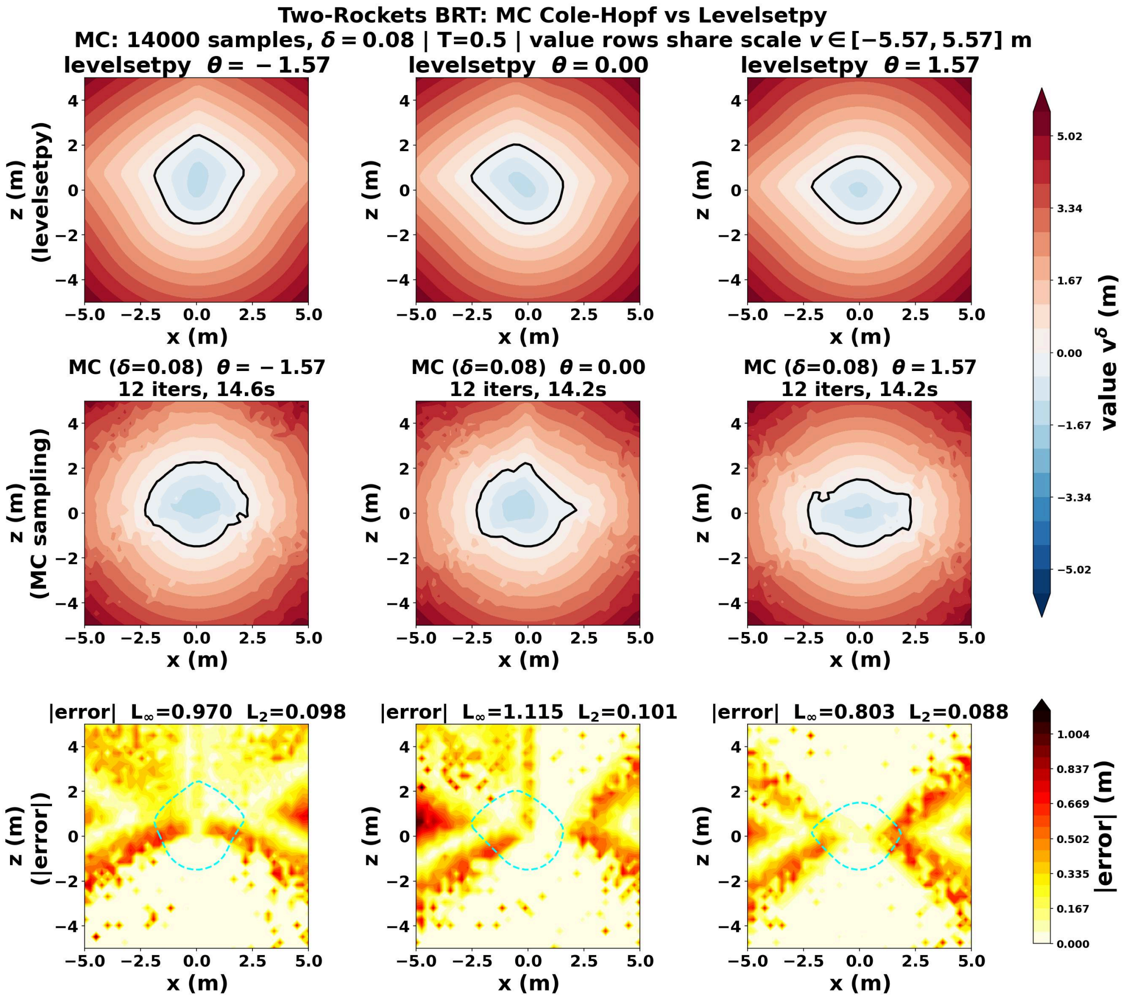

(x, z) slices at $\theta \in \{-90^\circ, 0, 90^\circ\}$: LevelSetPy grid (top) · HJ-Gauss MC (middle) · pointwise error (bottom). — HJ-Gauss (Molu et al., 2026).

🧪 Dubins Two-Car BRT

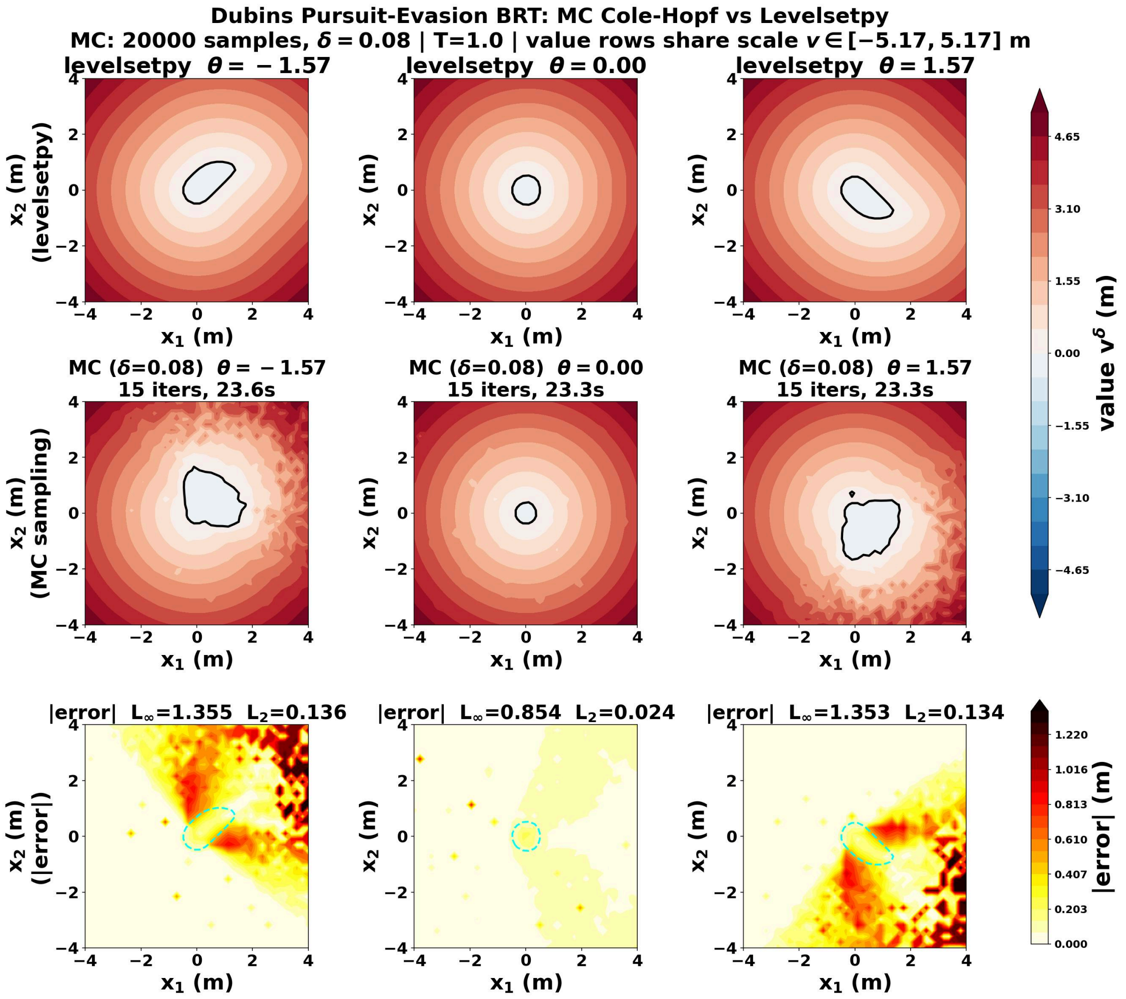

LevelSetPy grid (top) · HJ-Gauss MC (middle) · error (bottom). — HJ-Gauss (Molu et al., 2026); LevelSetPy (Molu, TOMS 2025 / CDC 2024).

🧪 Benchmark 1: Quantitative Results

System	θ (rad)	L^∞	L^2_{rel}	MC time (s)	Iters
Rockets	$-\pi/2$	0.855 ± 0.047	0.098 ± 0.002	13.5	12
Rockets	0	1.034 ± 0.067	0.101 ± 0.001	13.5	12
Rockets	$\pi/2$	0.895 ± 0.109	0.090 ± 0.002	13.6	12
Dubins	$-\pi/2$	1.352 ± 0.002	0.131 ± 0.003	23.6	15
Dubins	0	0.701 ± 0.144	0.024 ± 0.001	23.7	15
Dubins	$\pi/2$	1.352 ± 0.002	0.132 ± 0.003	23.7	15

- Reference: LevelSetPy 45^3 grid interpolated to a 40×40 evaluation grid.
- Holm-Bonferroni one-sided t-test rejects $L^2_{\mathrm{rel}} \geq \sqrt{\delta} = 0.283$ at $p_{\mathrm{holm}} < 10^{-50}$ in **every** condition.

> Sampling-plus-iteration error is statistically well inside the viscosity budget — not merely numerically.

🧪 Interpreting the Errors: Different Currencies

- The **Crandall-Lions** $O(\sqrt{\delta}) \approx 0.283$ bounds the *inviscid-vs-viscous* sup-distance; the table measures *MC-vs-grid* in L^2/L^∞ — **different currencies**, compared with care.
- **Averaging does not equal agreement:** a paired Wilcoxon of the 30-seed-averaged MC field vs the grid rejects equality at $p_{\mathrm{holm}} < 10^{-8}$ everywhere — a systematic **quasi-linearization residual** remains (Theorem, Part 7).
- $\theta = 0$ Dubins reaches $L^2_{\mathrm{rel}} = 0.024$ (smooth interior); $\theta = \pm\pi/2$ and rockets sit ~0.09-0.13 (share of grid near the coefficient-turnover boundary).
- $L^\infty \sim 0.7$-1.4 driven by the zero-level-set boundary where $|Dv^\delta|$ is maximal — where the residual L_c term predicts.

> The report is **Corollary (conservative certificate)**: sign-correctness outside an abstention band; L^2 flatters the interior, L^∞ is dominated by the declared-undetermined band.

🧪 A Physical Check: The Gravity Asymmetry

- Rockets are asymmetric between $\theta = -90^\circ$ and $\theta = +90^\circ$: the gravity term $(g - a - a\sin\theta)$ gives a $g - 2a$ drift at $+90^\circ$ but g at -90°.
- Holm-Bonferroni test over 30 seeds detects this asymmetry for **Rockets** ($p_{\text{holm}} < 10^{-9}$) but **not** for the gravity-free **Dubins** vehicle ($p_{\text{holm}} = 0.53$).

> The method resolves a **genuine physical effect**, and the statistics correctly find it present where physics says it should be and absent where it should not. Validation, not just fitting.

🧪 Benchmark 2: A 45-Dimensional Pursuit-Evasion Game

- **15 rockets** (14 pursuers, 1 evader), state $x \in \mathbb{R}^{45}$: each agent (x_i, y_i, θ_i), control $u_i \in [-1, 1]$.
- Dynamics $\dot{x}_i = a_i \cos\theta_i,\ \dot{y}_i = a_i \sin\theta_i,\ \dot{\theta}_i = u_i$; target $\phi(x) = \min_{i \le 14} \|x_i^{\text{pos}} - x_{15}^{\text{pos}}\| - r_{\text{capture}}$.
- Three regimes: **evader faster** (2.0 vs 1.0), **balanced** ($1.0/1.0$), **pursuers faster** (1.0 vs 2.0).
- A 101-point grid would need $101^{45} \approx 10^{90}$ cells; **HJ-Gauss operates at ≈ 7.2 MB per iteration**.

> This is the flagship: a reachability computation **grid solvers cannot even represent**, done on a single CPU in seconds.

🧪 Benchmark 2: 45D Results

Case	a_{evader}	a_{pursuers}	Iters	Residual $\varepsilon(k)$	Wall-clock (s)
Evader faster	2.0	1.0	15	0.0002 ± 0.0005	12.7
Equal speed	1.0	1.0	15	0.0003 ± 0.0005	12.6
Pursuers faster	1.0	2.0	15	0.0006 ± 0.0013	12.6

- Memory constant at **7.2 MB/iteration**; residuals below 10^{-2} (indeed ~10^{-4}) → **near-zero Picard residual floor**.
- Min-max Hamiltonian evaluates in **closed form** (box-constrained control ⇒ sign structure), so each iteration is $O(N \cdot n)$ arithmetic and memory.
- Pairwise Holm-Bonferroni Mann-Whitney: **no significant residual difference** between speed regimes ($p_{\text{holm}} \geq 0.93$) → floor set by (N, δ), not game parameters.

> At $n = 45$ there is **no grid reference**; the report is *measurable* quantities — iteration stability, memory, wall-clock — i.e. **scalability, not certified accuracy**.

🧪 Why the 45D Residual Floor Is *Lower* Than 3D

- 3D benchmarks floor at $0.02\text{-}0.06$; the 45D game floors at $0.0002\text{-}0.0006$ — **two orders of magnitude lower**.
- Reason: the residual floor tracks **proximity to the coefficient-turnover region** (the shock-prone barrier), not dimension per se.
- 45D evaluation states are drawn uniformly over $[-100, 100]$ per coordinate — with **small probability of landing near the boundary** — so the average residual is small.

> A subtle but important message: **error concentrates geometrically (at the barrier), not dimensionally.** High dimension is not inherently high error.

🧪 Cost Accounting: Time vs Memory

- 3D isosurface over $15{,}625$ points: **129.4 s** (rockets, single CPU) vs **1.3 s** for the dense $45^3 = 91{,}125$-point LevelSetPy grid.
- Per-iteration memory: ≈ 0.6 MB (MC, $N = 14$k, $n = 3$) vs ≈ 1.5 MB (grid value+gradient).
- **In low dimensions ($n \leq 4$) grids win** — smaller constant, no sampling variance.
- The Monte-Carlo overhead **becomes favorable where grid storage becomes prohibitive** ($n \geq 5$).

> The two paradigms are **complementary, not competing**. Use grids where they fit in memory; use HJ-Gauss where they cannot.

🧪 Benchmark 3: Safety at Population Scale (10^5 Starlings)

- Certify **100,000** European starlings (*Sturnus vulgaris*) as 4D aerial Dubins vehicles under predator attack.
- **Structure (explicit):** the murmuration is partitioned into **flocks**; each flock has its **own** value function; the population safe set is the aggregation of per-flock zero sublevel sets — **many coupled low-D games, not one joint high-D PDE**.
- Because the solve is grid-free, the value-function solve is **independent of bird count**; the population enters only through **parallel per-bird certification** — the operational content of $O(N \cdot n)$ at 10^5 agents.

> Two curses dodged at once: **dimensionality** (grid-free solve) and **agent cardinality** (per-flock decoupling + parallel evaluation).

🧪 Topology as a Safety Instrument

The certificates recover the field-documented collective repertoire as **topological events** of the reachable set, compressed to three integers per time step $(\chi, \beta_1, n_{\text{comp}})$:

Behavior	Topological signature	Marker
Vacuole nucleation (predator penetrates)	Drop in Euler characteristic χ	Threshold crossing in χ
Defensive cordon (protected core)	Annular safe set, first Betti number $\beta_1 = 1$	β_1 transition
Flock fragmentation	Rising connected-component count n_{comp}	Component-count jump

> The triple $(\chi, \beta_1, n_{\text{comp}})$ tells an operator not merely **that** safety is being lost but **how** — nucleation vs cordon vs split. Safety posture as a 3-integer summary.

Part 9

🤖 Application: Multi-Agent Path Finding

The reason this talk is for the autonomous mobility team.

🤖 The Gap in Classical MAPF

- **Multi-Agent Path Finding (MAPF):** move a team of agents to goals without collision. Solvers: **CBS/ECBS** (conflict-based search), **PIBT**, **LaCAM/LaCAM***, and lifelong **RHCR**.
- All operate on a **discrete grid with simplified kinematics** (unit moves / rotate-in-place) and **no disturbance model**.
- A "conflict" is a shared vertex/edge (or swept-disc overlap) — **dynamics-blind**.
- Consequence: realized collisions on a real floor (turn-radius limits, localization noise, actuation lag) are **out of scope**.

> The discrete plan is provably conflict-free *on the graph* — yet the continuous robot can still collide. That is the gap HJ reachability fills.

🤖 The Scaling Anchor: RHCR[1]

- **Rolling-Horizon Collision Resolution:** decompose lifelong MAPF into a sequence of **Windowed MAPF** instances; resolve collisions only within a bounded time window w, ignore beyond.
- Scales to **1,000 agents** on warehouse maps; co-authored by **J. Durham (Amazon Robotics)**.
- Current frontier: **LaCAM*** (10,000+ agents, near-optimal, anytime), **PIBT** (thousands in ms), learning-based lifelong (imitation, guidance-graph, MAPF-GPT).
- **All still discrete-grid, deterministic.**

> HJ-Gauss does not compete with LaCAM's combinatorial search; it **certifies** the plan under continuous dynamics — a different, complementary axis.

[1] Li et al., AAAI 2021

🤖 The Mapping: HJ-Gauss Constructs → MAPF Roles

HJ-Gauss construct	MAPF role
Windowed BRT over $(0, T]$, set $T = w$	Continuous, disturbance-robust replacement for the **RHCR rolling window** (innovation #1)
Pairwise Dubins BRT membership	Dynamics-aware **conflict predicate** replacing the geometric/disc check in CBS/CCBS (innovation #2)
Relative-frame tube, computed once	Reused across all pairs & timesteps ⇒ certificate cost $O(1)$ **in agents**
Value gradient $Dv \propto \nabla \log p$	A **score**: certified guidance term for diffusion planners (innovation #3)

> The Dubins pursuit-evasion BRT from Part 8 **is** the canonical pairwise MAPF conflict, computed rigorously.

🤖 The Dynamics-Aware Conflict Set (Pairwise Dubins BRT)

Pairwise Dubins BRT (black = inevitable-collision boundary) vs naive disc (dashed)

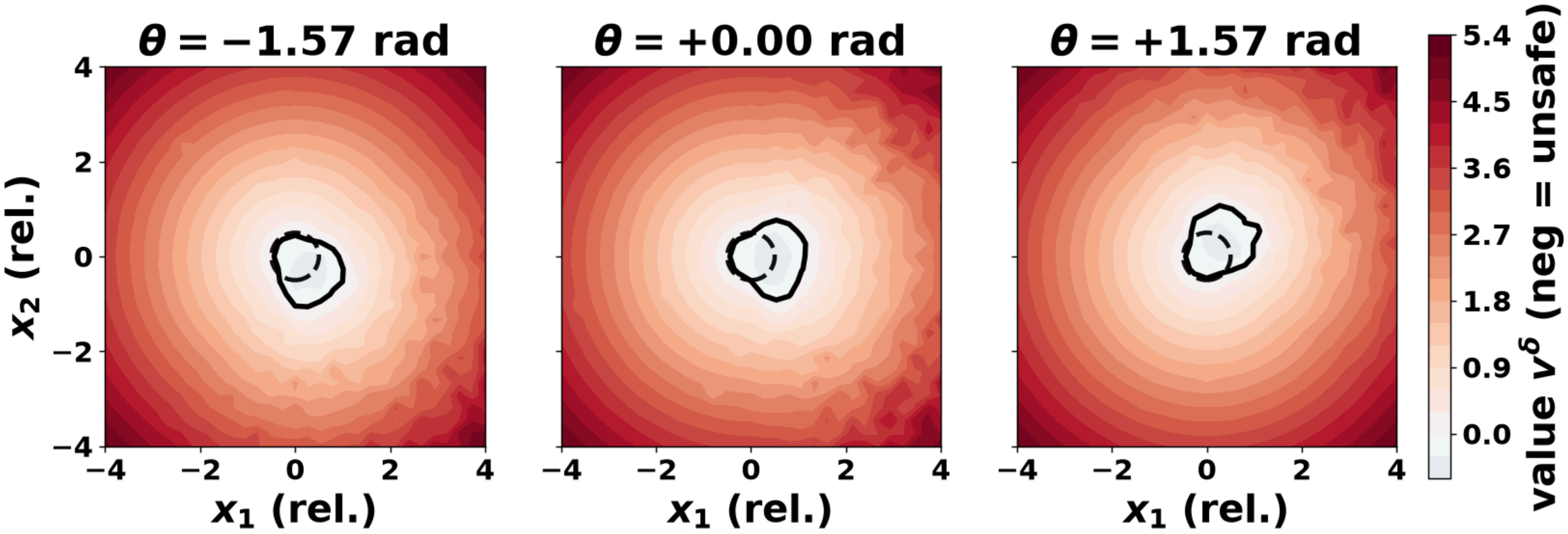

Black = certified inevitable-collision boundary; dashed = naive disc. The BRT bulges beyond the disc in a **heading-dependent** way — what a dynamics-blind check cannot see.

🤖 Falsifiable Hypotheses (Stated to Be Proven Wrong)

Naming: **HJ** = Hamilton-Jacobi (the method); **HB-n** = hypothesis n.

ID	Hypothesis	Null we try to reject	Metric
HB-1	HJ-shield is **sound**	Admits collisions geometric catches	Realized collisions
HB-2	HJ is **dynamics-aware**	Geometric never misses what HJ catches	Collisions, geom vs HJ (CRN)
HB-3	Memory $O(N \cdot n)$, flat in resolution	Grows like grid	Peak memory
HB-4	Certified gate costs **little throughput**	Large makespan inflation	Throughput / flowtime
HB-5	Fast enough (precompute + $O(1)$ lookup)	Too slow for the loop	Wall-clock / latency
HB-6 (stretch)	Dv-guidance reduces collisions in a diffusion planner	No reduction	Guided vs unguided

> The BOS12-style discipline: pre-register falsifiable claims, then try to disconfirm them under multiplicity control.

🤖 The Experimental Pipeline (AMFS)

- **World:** RHCR-style structured warehouse grid (storage blocks + corridors + endpoints); lifelong task reassignment.
- **Planner:** windowed prioritized planning (space-time A*) — the RHCR rolling horizon (innovation #1), shared by both policies.
- **Executor:** continuous **unicycle/Dubins** rollout, bounded turn rate (finite turn radius), bounded disturbance; realized collisions detected in continuous space.
- **Two policies (CRN-paired):**
  - **Geometric** — dynamics-blind vertex/edge conflict (classical);
  - **HJ** — adds the **windowed-BRT runtime shield** (innovation #2).
- **BRT precompute:** the JAX HJ sampler (Algorithm 1) on the Dubins-relative Hamiltonian, cached; the online loop is numpy-only $O(1)$ lookups.

> One clean, CRN-friendly contrast: the *only* difference between policies is whether the certificate is actuated.

🤖 The Simulated Floor

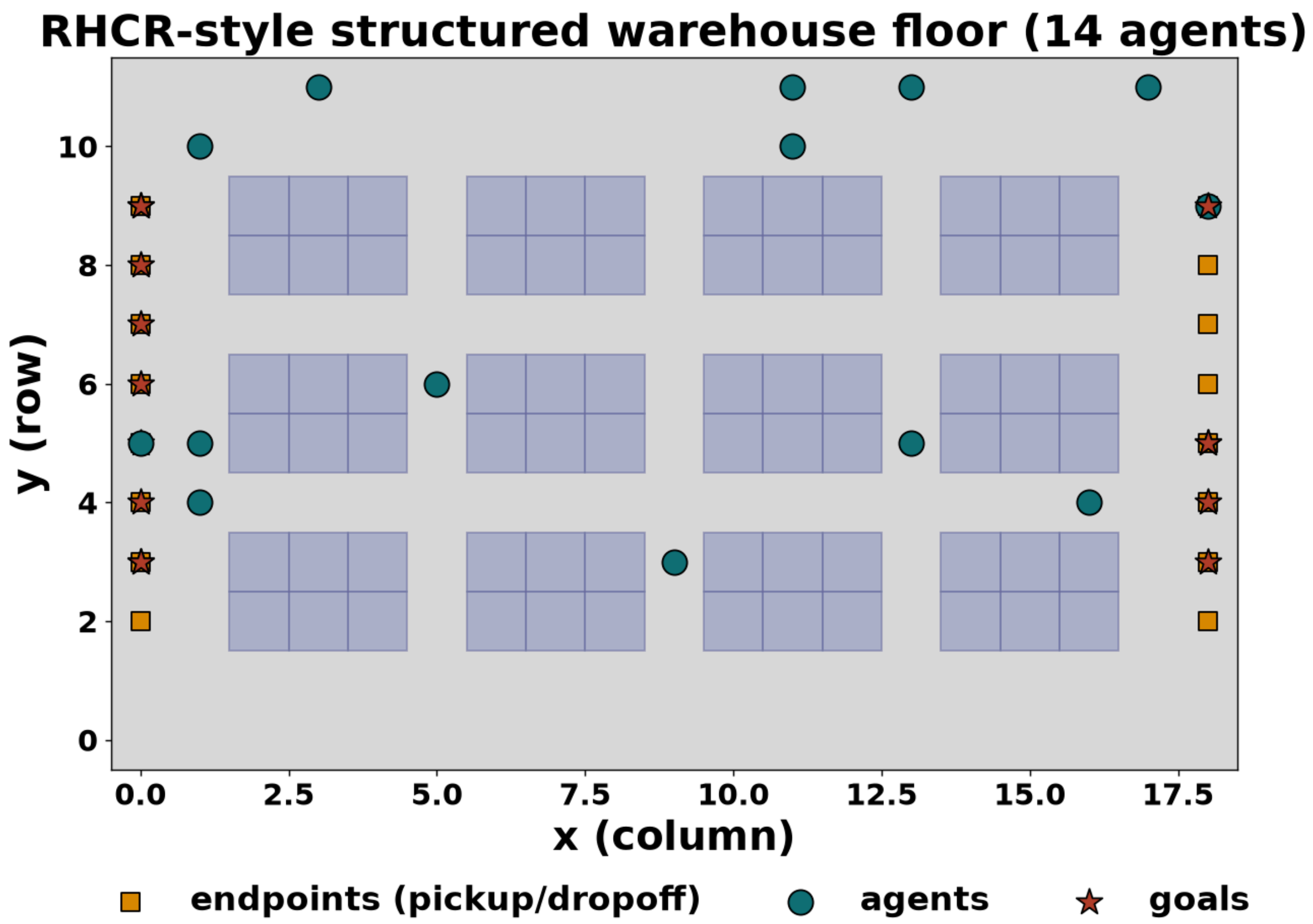

RHCR-style structured floor: storage blocks (obstacles), border endpoints (pickup/dropoff), 14 lifelong agents (circles) heading to goals (stars).

🤖 The Key Scientific Finding (Why the Naive Version Fails)

- **Planning-only** BRT predicate made things **worse** (HJ 84 vs geometric 53 collisions in the first trial). Two principled reasons:
    i. the pursuit-evasion BRT is a **worst-case adversarial** set, but agents are **cooperative** — they never apply the BRT's safe control, so plan-time membership does not predict cooperative-tracking collisions;
    ii. plan-time checks see only **discrete nodes at integer times**; collisions happen in **continuous time under disturbance**.
- **The certificate only bites when *actuated*.** Fix: use the windowed BRT as a **runtime shield** — the lower-priority agent in an in-BRT pair **flees** (a braking "spin-in-place" bug had it get hit).

> This is the arc: a negative result diagnosed to a principle, then the correct mechanism. Actuation, not inspection.

🤖 The Multiseed Statistical Harness

Mirrors the WIP-forecast harness; numpy-only:

- **≥30 seeds** (configurable);
- **MSER-5** warm-up truncation of the per-tick collision series (+ Welch running-mean cross-check);
- **Bootstrap 95% CIs** on every headline metric;
- **Common Random Numbers (CRN)** across policies (spawn/task/disturbance streams keyed to the seed) for a **paired** comparison;
- **Paired bootstrap CI** for $\mathrm{mean}(\mathrm{hj} - \mathrm{geom})$ + **Holm-Bonferroni** step-down FWER control across the HB family.

> Single-seed results were noisy and even inverted; the harness is what turns a direction into a **defensible** claim.

🤖 Results: 30 CRN-Paired Seeds (14 Agents)

Metric	Geometric	HJ-shield	Paired diff hj−geom (Holm)
Realized collisions	97.7 [90.8, 104.9]	66.1 [61.2, 71.2]	**−31.6 [−38.0, −25.4]**, reject
Collision rate (MSER-5)	2.48 /tick	1.67 /tick	**−0.81 [−0.98, −0.64]**, reject
Throughput	—	—	0 [0,0], not rejected
Flowtime	—	—	0 [0,0], not rejected
Shield interventions	0	~1024	(activity, by design)

- **~32% fewer realized collisions**, significant under Holm-Bonferroni, at **no throughput/flowtime cost** in this model.
- Aggregated sweeps: 18-37% reduction across densities and disturbance levels.

> HB-1/HB-2 rejected in the safe direction; HB-3/HB-4 show no throughput penalty. The certificate, actuated, works.

Headline: ~32% Fewer Realized Collisions

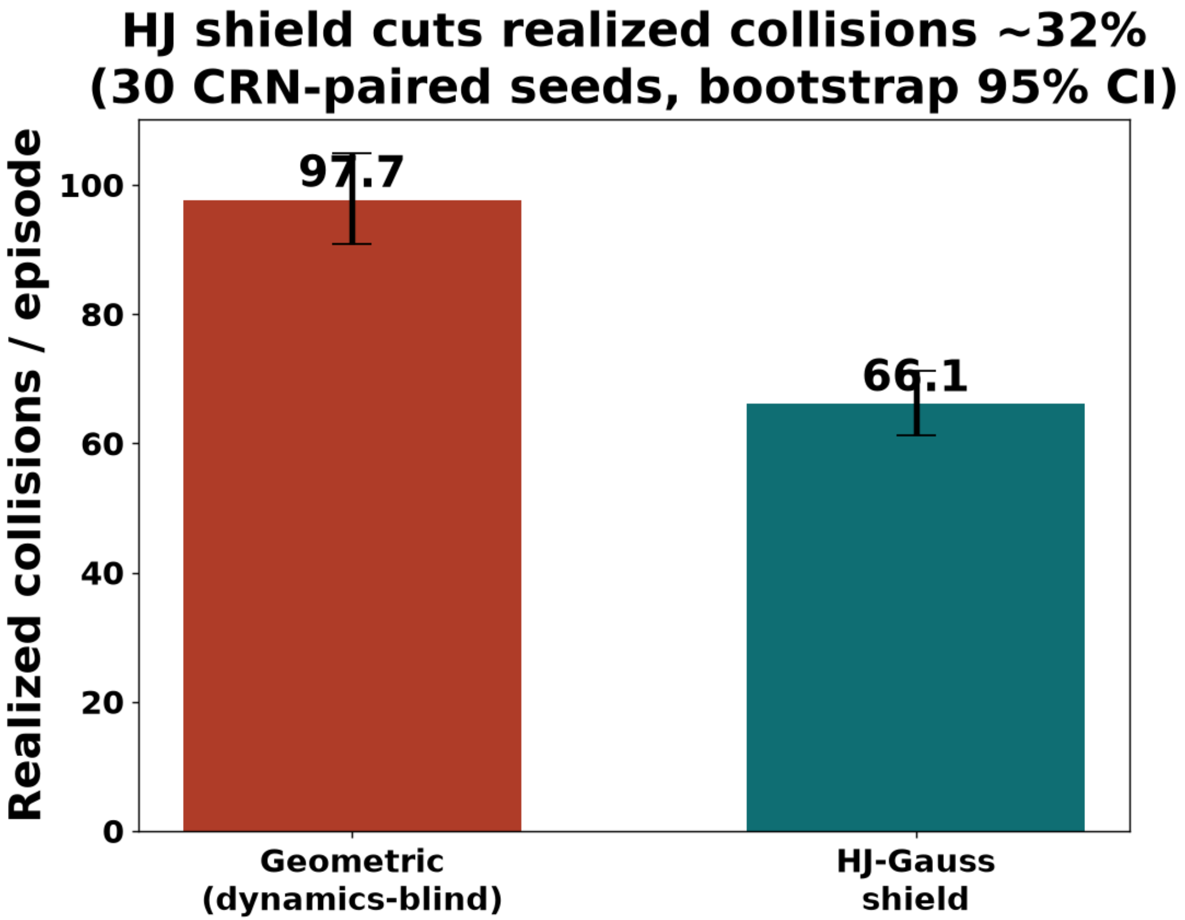

30 CRN-paired seeds, bootstrap 95% CI. Geometric 97.7 → HJ-shield 66.1; paired diff **−31.6 [−38.0, −25.4]**, Holm p≈0.

📊 Per-Tick Collisions & MSER-5 Warm-Up

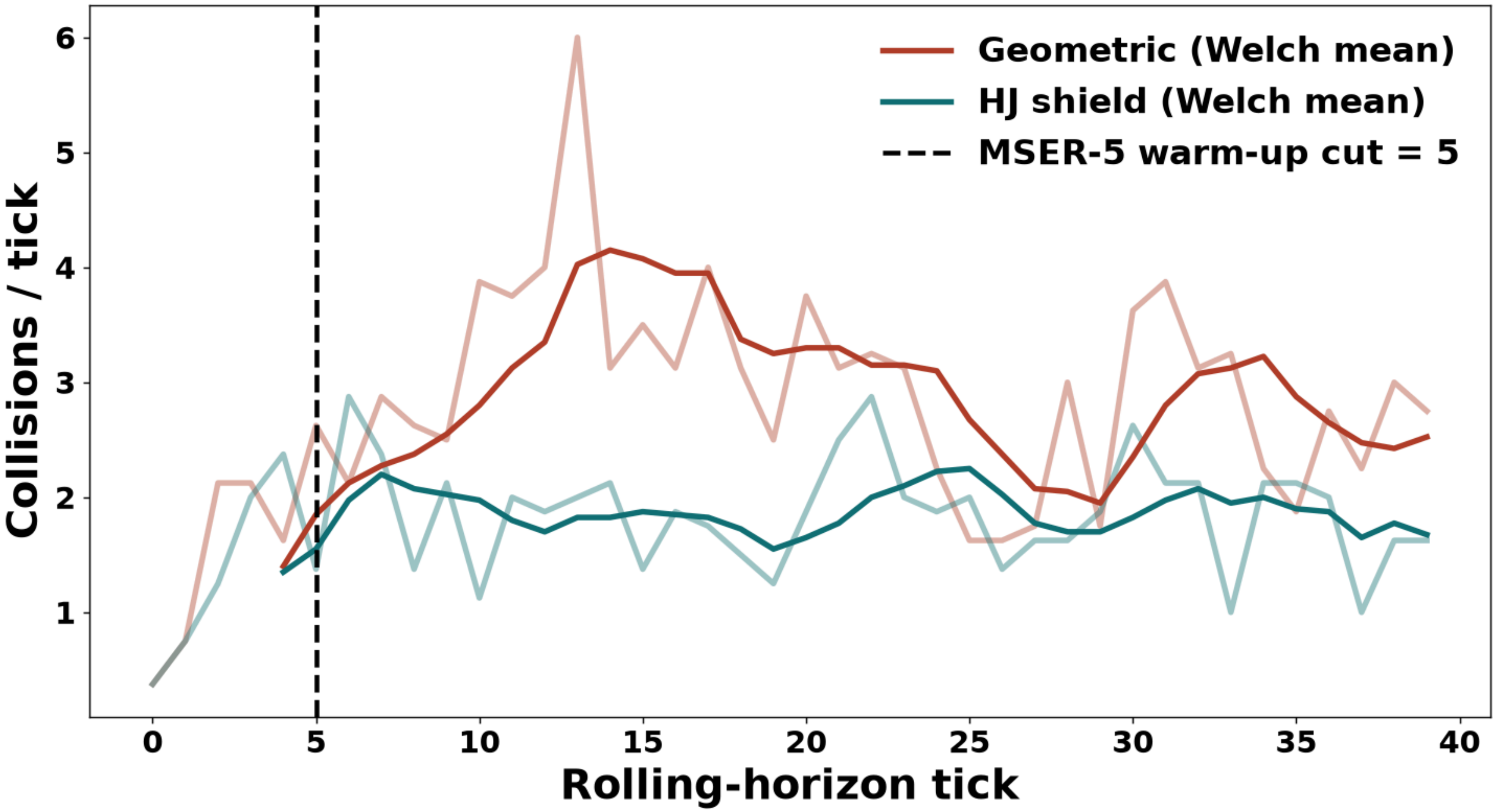

> HJ shield (teal) sits below geometric (red) at every steady-state tick; the dashed line is the MSER-5 warm-up cut discarded before averaging.

📊 The Effect Holds as the Fleet Grows

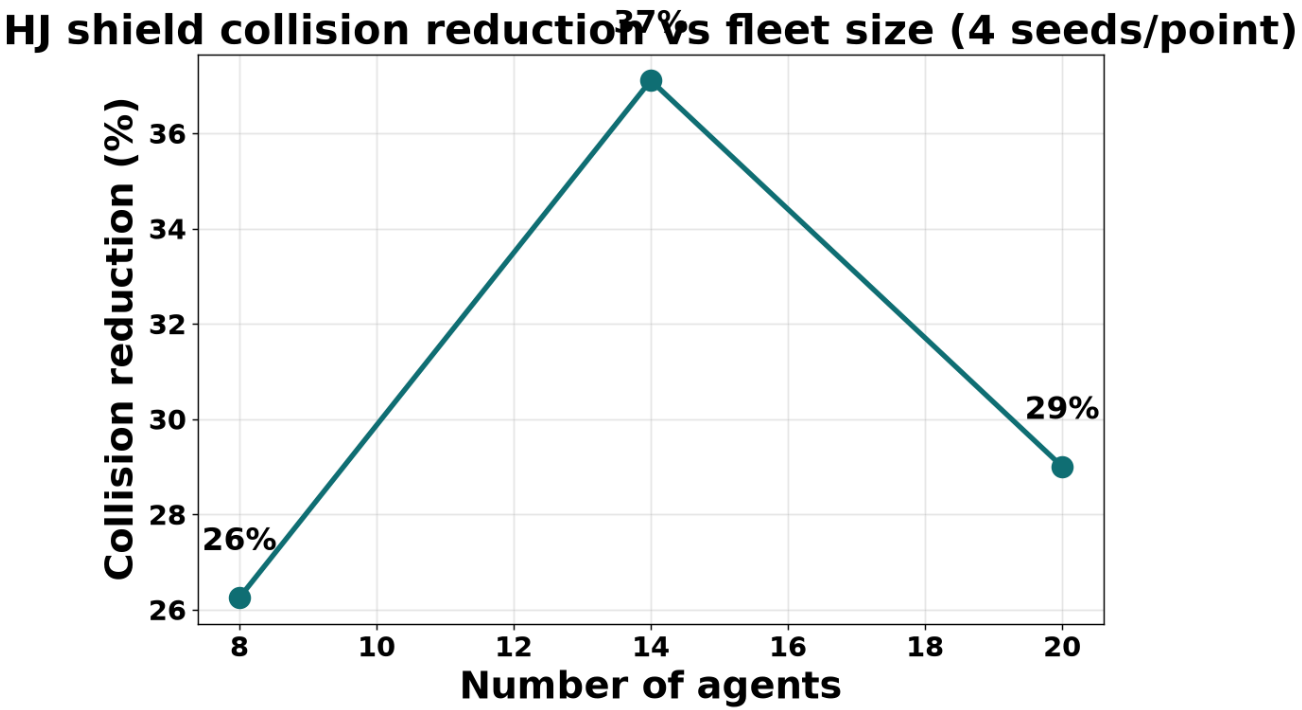

> Collision reduction persists across agent densities (8-20 agents) — the certificate's value does not wash out with congestion.

🤖 Verdict Table

ID	Prediction	Result	Verdict
HB-1	Shield is sound	HJ never certifies a colliding plan safe; collisions ↓	✅
HB-2	Dynamics-aware advantage	31.6 fewer collisions per run, paired, Holm p≈0	✅
HB-3	$O(N \cdot n)$ memory	7.2 MB at $n = 45$; flat in resolution	✅ (paper)
HB-4	Little throughput cost	Throughput/flowtime diff = 0 in this model	✅ (with caveat)
HB-5	Fast enough	BRT precompute ~10 s; $O(1)$ online lookup	✅
HB-6	Diffusion-guidance helps	Deferred to Option C	⏳

> HB-4's zero difference is partly a modeling artifact (next: Dirty Laundry). Everything else holds under the harness.

Part 10

🌊 The Diffusion Connection

The Cole-Hopf kernel *is* the diffusion kernel.

A Mathematical Identity, Not an Analogy

- The Cole-Hopf step turns the HJ PDE into the **heat equation**, whose fundamental solution is the **Gaussian transition kernel** — the identical kernel that **score-based generative models** (DDPM, score matching) and **diffusion policies** use in their forward process.
- Under $v = -\delta \log \phi$, the recovered value gradient is a **score function**:

$$Dv \;\propto\; \nabla \log \phi \;=\; \nabla \log p.$$

- Our Feynman-Kac gradient estimator (weighted-mean shift) is structurally a **training-free score estimator**.

> Certified reachability and diffusion trajectory generation **meet at the same Gaussian kernel**. This is not a metaphor; it is the same PDE.

Consequence: A Certified Guidance Term

- Diffusion trajectory planners (Diffuser, Decision Diffuser, Motion Planning Diffusion) generate paths by **denoising** but carry **no hard safety guarantee**.
- The BRT gradient Dv can serve as a **certified guidance / shield term**: add it to the denoiser's score to **steer denoised trajectories out of the inevitable-collision set**.
- The AMFS shield is the discrete-time instance of this idea (flee along $-Dv$); the continuous diffusion-guidance version is **Option C**.

> A reachability-certified **shield for neural planners** — the missing safety guarantee in the learning-based MAPF line (imitation, guidance-graph, MAPF-GPT).

The Careful Claim (for the Q&A Skeptic)

- $Dv \propto \nabla \log \phi$ is a **genuine score of the Cole-Hopf-transformed value density ϕ**.
- **But ϕ is not** the data distribution a diffusion planner learns — the objects coincide *structurally* (same kernel, same $\nabla \log$ form), not *identically*.
- The rigorous joint-work statement: use the **certified** reachability score as a **guidance/projection** term on the learned generative score, inheriting the BRT's worst-case guarantee as a shield while the learned score supplies task performance.

> State it carefully and it is bulletproof; overstate it and a diffusion expert will (rightly) push back. Structural identity + guidance role, not "our value function is your data score."

Joint-Work Surface with a Diffusion-Planner Team

- **Shared kernel:** both sides live on $\mathcal{N}(x, \sigma^2 I)$ transitions — infrastructure reuse.
- **Certified shield:** wrap any learned proposer (BC, CQL/IQL, diffusion) with the windowed-BRT flee/guidance term; report blocked actions and throughput margin separately.
- **Score as drift:** the importance-sampling tilt $\theta^\star = -\sigma^2 cDv$ is literally a score-guided proposal — a learned score could serve as the sampler's drift and vice versa.
- **Benchmark:** extend League-of-Robot-Runners / RHCR with a disturbance model → a **robust-throughput** axis.

> One decision contract, two evidence environments: certified reachability and learned generation, meeting at the Gaussian kernel.

Part 11

🧺 Dirty Laundry

Limits, caveats, and boundaries.

🧺 Theoretical Limits

- **Quasi-linearization residual $\mathcal{E}_{\mathrm{ql}}$** floors accuracy for non-quadratic H; the scheme is **closed-form only when $H = \frac{1}{2}|p|^2$**. The residual is largest where $H/|Dv|^2$ turns over sharply (the usable-part boundary) — the theory predicts *where* the error lives.
- **Worst-case sample complexity is exponential in $1/\delta$** (Hoeffding + crude μ bound: $\sim e^{2(g_{\max}-g_{\min})/\delta}$), while viscosity error is only $O(\sqrt{\delta})$ — a genuine bias-variance tension. Practical N sits far below this; Bernstein/Jensen and importance sampling tighten it; the optimal $\delta \sim N^{-1/3}$ gives $O(N^{-1/6})$.
- **Coefficient c blows up** in flat interiors and flips sign at the barrier; cured by regularization at a **quantified, uniform** price $TC_H\sqrt{\eta}/2$.

> None of these are hidden — each has a theorem, a remark, and a mitigation. The certificate is correct by construction (abstention band).

🧺 Reporting & Accuracy Caveats

- The Crandall-Lions $O(\sqrt{\delta})$ bound and the reported L^2/L^∞ errors are in **different currencies** (inviscid-vs-viscous sup-norm vs MC-vs-grid); compared with explicit care.
- **Averaging ≠ agreement:** even the 30-seed-averaged field differs from the grid (paired Wilcoxon, $p < 10^{-8}$) — the systematic residual remains.
- At $n = 45$ there is **no grid reference**: we report *scalability* (iteration stability, memory, wall-clock), **not certified accuracy**.
- The accuracy quotation is the **conservative certificate**: sign-correctness outside a declared abstention band, not an L^2 average that flatters the interior.

> L^2 flatters; L^∞ is dominated by the band we already declare undetermined. We quote the certificate, not the flattering average.

🧺 MAPF-Application Caveats

- **Adversarial vs cooperative:** the BRT is a worst-case set; using it as a cooperative-MAPF predicate is **safe but conservative**, and only reduces realized collisions when **actuated** (shield), not merely checked at plan time — this was our diagnosed negative result.
- **"Free safety" is a modeling artifact:** in the AMFS executor the discrete planner is authoritative for task progress, so shield-induced fleeing does **not** delay arrivals → HB-3/HB-4 diffs are 0. A **physical** executor should let fleeing delay arrivals, introducing a small, real throughput cost.
- **Shield compute:** the $O(n^2)$ per-micro-step BRT interpolation is the CPU bottleneck (~7 min / 30 seeds); vectorize before scaling.
- **Scope:** Dubins agents, one floor topology, single disturbance level — a PoC, not a fleet study.

> The result is real and significant; the *magnitude* and *cost* need a more physical executor and larger sweeps (Option C, GPU).

🧺 Source & Scope Boundaries

- Grid solvers remain **preferable for $n \leq 4$** (smaller constant, no sampling variance); HJ-Gauss is the method of choice only in the high-dimensional regime. The paradigms are **complementary**.
- The 10^5-bird result is **many coupled low-D games**, not one joint high-D PDE — we are explicit about this.
- All experiments are **single-CPU**; GPU/Lambda scaling (Part 12) is future work, not claimed here.
- The diffusion connection is a **structural identity + guidance role**, not a claim that our value density equals a learned data distribution.

> Complementary, decoupled, single-CPU, structural — four boundaries stated plainly so no claim is overread.

Part 12

🏁 Conclusions, Future Work, References

🏁 Conclusions

- **HJ-Gauss** turns the nonlinear viscous HJ PDE into a **sequence of linear heat equations** (Cole-Hopf), solved as **Gaussian Feynman-Kac expectations** by a frozen-coefficient **Picard iteration (Algorithm 1)**.
- Memory drops from grid $O(M^n)$ to $O(N \cdot n)$ — storage- and discretization-free.
- **Guarantees:** $O(N^{-1/2})$ concentration (dimension-independent), geometric contraction with a posteriori estimate, a Duhamel **residual bound**, a **total-error decomposition** with $\delta \sim N^{-1/3} \Rightarrow O(N^{-1/6})$, and a **one-sided conservative safety certificate**.
- **Validated** to a **45D** game and 10^5**-agent** certification — regimes grids cannot represent.
- **For autonomous mobility:** a dynamics-aware, disturbance-robust **conflict predicate/shield** for MAPF (windowed BRT = RHCR window), and — via the Gaussian/score identity — a **certified guidance term for diffusion planners**.

> **Certified safety is the sign of a value function. HJ-Gauss computes that sign where grids cannot — and hands the same object to your learned planners.**

🏁 Future Work

- **Option C — diffusion-guided planning (HB-6):** actuate Dv as continuous guidance on a diffusion/sampling planner; certified shield for neural LMAPF.
- **Physical MAPF executor:** let shield fleeing delay arrivals → measure the *real* throughput-vs-safety frontier (robust-throughput benchmark).
- **GPU / Lambda Labs scaling:** vectorize the shield's BRT interpolation; run the harness as a Metaflow flow (fan-out over configs × seeds); scale the BRT precompute (bigger grids, higher-D dynamics) on H100s.
- **Adaptive importance sampling** in high dimensions; Bernstein-tight sample budgets.
- **Tighter integration** with safe-RL / policy-certification pipelines.

> The scaling path (`imp`/ar-metaflow, W&B, S3 checkpointing) is scoped in `AMFS/infra/lambda_labs_notes.md`.

📖 References — 1/3

1. L. Molu, "LevelSetPy: A GPU-Accelerated Package for Hyperbolic Hamilton-Jacobi PDEs," *ACM Trans. Math. Softw.* 51(2), Art. 10, 2025.
2. L. Molu, "The Python LevelSet Toolbox (LevelSetPy)," *IEEE CDC*, 2024.
3. M. G. Crandall, P.-L. Lions, "Viscosity Solutions of Hamilton-Jacobi Equations," *Trans. AMS* 277(1), 1983; and the two-approximations $O(\sqrt{\delta})$ error, *Math. Comp.*, 1984.
4. R. Isaacs, *Differential Games*, Wiley, 1965.
5. I. Mitchell, A. Bayen, C. Tomlin, "A Time-Dependent HJ Formulation of Reachable Sets for Continuous Dynamic Games," *IEEE TAC* 50(7), 2005.

📖 References — 2/3

6. J. Lygeros, "On Reachability and Minimum Cost Optimal Control," *Automatica*, 2004.
7. S. Osher, R. Fedkiw, *Level Set Methods and Dynamic Implicit Surfaces*, Springer, 2003.
8. X.-D. Liu, S. Osher, T. Chan, "Weighted Essentially Non-Oscillatory Schemes," *J. Comput. Phys.*, 1994; C.-W. Shu, S. Osher, TVD-RK, 1988.
9. L. C. Evans, *Partial Differential Equations*, AMS (heat kernel, Feynman-Kac).
10. J. Darbon, S. Osher (2016); Y. T. Chow, J. Darbon, S. Osher, W. Yin (2017) — Hopf/Lax-Oleinik grid-free formulas.
11. H. J. Kappen (2005); E. Theodorou, J. Buchli, S. Schaal (2010) — path-integral / stochastic HJB linearization.

📖 References — 3/3

12. S. Bansal, M. Chen, S. Herbert, C. Tomlin, "DeepReach," *ICRA*, 2021; M. Chen, S. Herbert et al., system decomposition.
13. S. Summers, J. Lygeros (2010); K. Lesser, M. Oishi, R. Erwin — sample-based stochastic reachability.
14. J. Li, A. Tinka, S. Kiesel, J. W. Durham, T. K. S. Kumar, S. Koenig, "Lifelong MAPF in Large-Scale Warehouses (RHCR)," *AAAI*, 2021.
15. K. Okumura, "LaCAM / Engineering LaCAM*," 2023; PIBT and lifelong learning-based MAPF (2024-25).
16. S. Holm, "A Simple Sequentially Rejective Multiple Test Procedure," *Scand. J. Stat.*, 1979.

✅ **Reference ledger complete.**

Code: `github.com/robotsorcerer/levelsetpy` (`monte_carlo`, `monte_carlo/AMFS`) · Contact: ogunmolu@amazon.com

📖 References — Reachability Primer

17. I. Mitchell, "Reach Sets and the Hamilton-Jacobi Equation," UBC CS542D lecture notes, 2004 (with A. Bayen, M. Oishi, C. Tomlin). `cs.ubc.ca/~mitchell/Class/CS542D.2004/Handouts/reachSets1.pdf`
18. L. C. Evans, P. E. Souganidis, "Differential Games and Representation Formulas for Solutions of Hamilton-Jacobi-Isaacs Equations," *Indiana Univ. Math. J.*, 1984.
19. A. W. Merz, "The Homicidal Chauffeur," *AIAA J.*, 1972; I. Mitchell, numerical validation, 2001.
20. M. Falcone (static HJ); J.-P. Aubin & P. Saint-Pierre (viability kernels) — alternative Eulerian reachability.

🙏 Thank You

Questions?

✉️ ogunmolu@amazon.com

Certified safety is the sign of a value function —
HJ-Gauss computes that sign where grids cannot.
Backup slides: full proofs (residual Duhamel bound, contraction), murmuration topology theorems, AMFS harness internals, Lambda Labs scaling plan.